STUDY OF THE UTILIZATION AND BENEFITS OF PHASOR MEASUREMENT UNITS FOR LARGE SCALE POWER SYSTEM STATE ESTIMATION

A Thesis

by

YEO JUN YOON

Submitted to the Office of Graduate Studies of
Texas A&M University
in partial fulfillment of the requirements for the degree of

MASTER OF SCIENCE

December 2005

Major Subject: Electrical Engineering

STUDY OF THE UTILIZATION AND BENEFITS OF PHASOR MEASUREMENT UNITS FOR LARGE SCALE POWER SYSTEM STATE ESTIMATION

A Thesis

by

YEO JUN YOON

Submitted to the Office of Graduate Studies of
Texas A&M University
in partial fulfillment of the requirements for the degree of

MASTER OF SCIENCE

Approved by:

Chair of Committee,	Ali Abur
Committee Members,	Chanan Singh
	Laszlo Kish
	Steven D. Taliaferro
Head of Department,	Chanan Singh

December 2005

Major Subject: Electrical Engineering

ABSTRACT

Study of the Utilization and Benefits of Phasor Measurement Units

for Large Scale Power System State Estimation. (December 2005)

Yeo Jun Yoon, B.S., Korea University, South Korea

Chair of Advisory Committee: Dr. Ali Abur

This thesis will investigate the impact of the use of the Phasor Measurement Units (PMU) on the state estimation problem. First, incorporation of the PMU measurements in a conventional state estimation program will be discussed. Then, the effect of adding PMU measurements on the state estimation solution accuracy will be studied. Bad data processing in the presence of PMU measurements will also be presented. Finally, a multi-area state estimation method will be developed. This method involves a two level estimation scheme, where the first level estimation is carried out by each area independently. The second level estimation is required in order to coordinate the solutions obtained by each area and also to detect and identify errors in the boundary measurements.

The first objective of this thesis is to formulate the full weighted least square state estimation method using PMUs. The second objective is to derive the linear formulation of the state estimation problem when using only PMUs. The final objective is to formulate a two level multi-area state estimation scheme and illlustrate its performance via simulation examples.

ACKNOWLEDGMENTS

First and foremost, I would like to express my deepest gratitude to Dr. Ali Abur for his guidance and encouragement. He has been a source of inspiration, throughout my graduate studies at Texas A&M University.

I would like to thank my committee members, Dr. Chanan Singh, Dr. Laszlo Kish and Dr. Steven D. Taliaferro, for their help. I would also like to acknowlege my professors at Texas A&M University from whom I have learned so much.

The work described in this thesis was sponsored by the Power Systems Engineering Research Center (PSERC). I also express my appreciation for the support provided by PSERC.

Finally, I would like to express my love and gratitude to my girl friend, Ara Cho , and my parents for their endless support and encouragement.

TABLE OF CONTENTS

Page

CHAPTER Page

LIST OF FIGURES

FIGURE Page

FIGURE Page

LIST OF TABLES

TABLE Page

CHAPTER I
INTRODUCTION

1.1 Modern Power System Operations

Over the twenty years, electric power industry in many countries has been undergoing fundamental changes due to the process of deregulation [1]-[4]. The belief is that competitive markets will lead to more efficient power generation, more technological innovations, and eventually to lower retail prices. In an interconnected system, there are multiple companies who must cooperate to run the system. Some companies may be reluctant to exchange their data for security concerns. In addition, the power system network is growing larger and more complex shared by more providers after the deregulation.

In this situation, the function of state estimation is becoming more important, because it is the primary tool for monitoring and control based on the real-time data received from the measurement units. As an example, one of the causes of Northeast blackout of 2003 was the poor control-room procedures and failure of power-grid organization to keep it from spreading [5]. The security analysis, economic dispatch, etc. strongly depend on the accuracy of data provided by the state estimation.

Recently, synchronized phasor measurement techniques based on a time signal of the GPS (Global Positioning System) are introduced in the field of power systems. In order to obtain simultaneous measurements of different buses it is necessary to synchronize sampling clocks at different locations. A PMU (Phasor Measurement Unit) which can increase the confidence in the state estimation result is practically introduced via the use of synchronized measurements [6]-[16]. Wide-area information from properly distributed PMUs enables the effective assessment of the dynamic performance of the power system and multi-area state estimation with independently operating system areas.

1.2 Multi-Area State Estimation Using PMUs

Since the start of the deregulation, power system operators are confronted with the

---

This thesis follows the style and format of *IEEE Transactions on Power Systems.*

need to monitor and coordinate power transactions taking place over large distances in remote parts of the power grid. Each operating center may have its own state estimator which processes the measurements given by its local substations. A system-wide state estimation solution is needed when the power transactions are involved in several control areas. A central state estimator will collect wide area measurements and will solve very large scale state estimation problem. However, solving the large scale state estimation is not easy. Other than the problem of huge size of the interconnnected system, each indepenent system operators may be reluctant to modify their existing system method in order to meet the new specifications imposed by the central state estimator for the large area solution. Then, a hierarchical multi-area state estimation is a solution for the individual system operators to keep their existing method and a central coordinator to determine the state of the overall system.

Synchronized phasor measurement units are indispensable to get a second level state estimation. PMUs can measure voltage and currents as phasors. The error is small compared with the conventional measurements such as power injection and power flow measurements. Until very recently, the measurements used by the multi-area state estimators typically included only synchronized voltage phasors from the PMUs. However, this thesis will include all the measured data from PMUs, such as voltage magnitudes and phasors and real and reactive part of currents.

1.3 Thesis Contributions

One of the contributions of this thesis is that it shows the effect of PMUs on the accuracy of variables. After showing how to implement the PMU measurement in state estimation, the effect is discussed by gradually increasing the PMU numbers. Four different kinds of IEEE Bus Systems are tested. Interesting thing is that the improved accuracy of variables are somewhat saturated when PMUs are implemented at nearly 10% of the total system buses. Second contribution of this thesis is the introduction of the linear formulated state estimation. There's no need to update the Jacobian matrix in state estimation algorithm when using only PMU measured data. Simulation example of the linearly

formulated state estimation and its bad data detection and identification process is illustrated. Lastly, this thesis presents a multi-area state estimation method including PMU measurements.

1.4 Organization of This Thesis

This thesis is composed of 6 chapters. Chapter I is the introduction. It shows the current problems and reviews the problem of state estimation. Chapter II presents the specific modeling and simulation method of the full weighted least square state estimation. Chapter III is the introduction of the linear formulation of the state estimation problem when using PMUs. Simulation works and bad data processing with the linear formulation are illustrated. Chapter IV shows the benefits of using PMUs. Improved accuracy of the estimated variables with PMUs is illustrated. Chapter V shows a multi-area state estimation method with PMUs. Firstly, current method of multi-area state estimation is reviewed, and proposed method is described. Then, the simulation results of the proposed multi-area state estimation method described. Finally, Chapter VI contains conclusions about this thesis and future work to make the state estimation method more applicable for real systems.

CHAPTER II
FULL WEIGHTED LEAST SQUARE STATE ESTIMATION

2.1 Introduction

Power system state estimation derives a real-time model through the received data from a redundant measurement set. Different kinds of methods about state estimation are reviewed in [17]-[19]. Among them, detailed weighted least squares(WLS) state estimation methods are shown in [20]-[23].

WLS state estimation minimizes the weighted sum of squares of the residuals. Consider the set of measurements given by the vector z:

$$z = \begin{bmatrix} z_1 \\ z_2 \\ \vdots \\ z_m \end{bmatrix} = \begin{bmatrix} h_1(x_1, x_2, \cdots, x_n) \\ h_2(x_1, x_2, \cdots, x_n) \\ \vdots \\ h_m(x_1, x_2, \cdots, x_n) \end{bmatrix} + \begin{bmatrix} e_1 \\ e_2 \\ \vdots \\ e_m \end{bmatrix} = h(x) + e \tag{2.1}$$

$h^T = [h_1(x), h_2(x), \cdots, h_m(x)]$

$h_i(x)$ is the nonlinear function relating measurement i to the state vector x

$x^T = [x_1, x_2, \cdots x_n]$ is the system state vector

$e^T = [e_1, e_2, \cdots e_m]$ is the vector of measurement errors.

Let $E(e)$ denote the expected value of e, with the following assumptions:

$$E(e_i) = 0\,,\ i = 1, \cdots, m \tag{2.2}$$

$$E(e_i e_j) = 0 \tag{2.3}$$

Measurement errors are assumed to be independent and their covariance matrix is given by a diagonal matrix R:

$$Cov(e) = E[e \cdot e^T] = R = diag\{\sigma_1^{\,2}, \sigma_2^{\,2}, \cdots, \sigma_m^{\,2}\} \tag{2.4}$$

The WLS estimator will minimize the following objective function:

$$J(x) = \sum_{i=1}^{m} (z_i - h_i(x))^2 / R_{ii} = [z - h(x)]^T R^{-1} [z - h(x)] \tag{2.5}$$

At the minimum value of the objective function, the first-order optimality conditions

have to be satisfied. These can be expressed in compact form as follows:

$$g(x) = \frac{\partial J(x)}{\partial x} = -H^T(x)R^{-1}[z - h(x)] = 0 \qquad \text{where, } H(x) = \left[\frac{\partial h(x)}{\partial x}\right] \tag{2.6}$$

The non-linear function $g(x)$ can be expanded into its Taylor series around the state vector x^k neglecting the higher order terms. An iterative solution scheme known as the Gauss-Newton method is used to solve (2.6):

$$x^{k+1} = x^k - \left[G(x^k)\right]^{-1} \cdot g(x^k) \tag{2.7}$$

where, k is the iteration index and x^k is the solution vector at iteration k.

$G(x)$ is called the gain matrix, and expressed by:

$$G(x^k) = \frac{\partial g(x^k)}{\partial x} = H^T(x^k) \cdot R^{-1} \cdot H(x^k) \tag{2.8}$$

$$g(x^k) = -H^T(x^k) \cdot R^{-1} \cdot (z - h(x^k)) \tag{2.9}$$

Generally, the gain matrix is quite sparse and decomposed into its triangular factors. At each iteration k, the following sparse linear set of equations are solved using forward/backward substitutions, where $\Delta x^{k+1} = x^{k+1} - x^k$:

$$\left[G(x^k)\right]\Delta x^{k+1} = H^T(x^k) \cdot R^{-1} \cdot \left[z - h(x^k)\right] = H^T(x^k) \cdot R^{-1} \cdot \Delta z^k \tag{2.10}$$

This iterations are going on until the maximum variable difference satisfies the condition, '$Max\left|\Delta x^k\right| < \varepsilon$'. A detailed flow-chart of this algorithm is shown in next section.

2.2 WLS State Estimation Algorithm

WLS state estimation uses the iterative solution of Equation (2.10). Iterations start at an initial guess x^0 which is typically chosen as the flat start, i.e. all bus voltages are assumed to be 1.0 per unit and in phase with each other. The flow-chart of the iterative algorithm for WLS state estimation problem can be outlined in Figure 1.

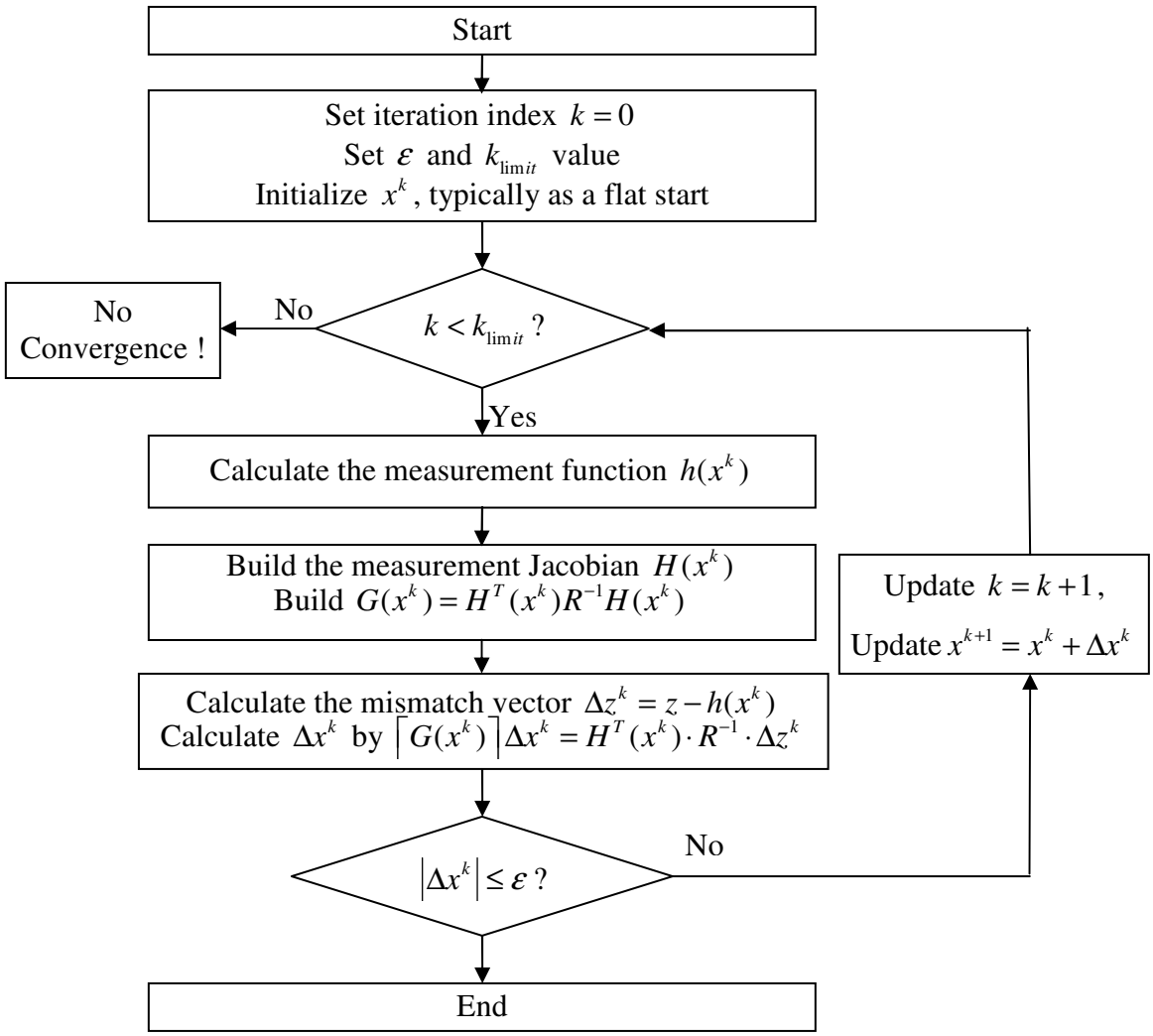

Figure 1. Flow-Chart for the WLS State Estimation Algorithm

1) Initially set the iteration counter $k = 0$, define the convergence tolerance ε and the iteration limit k_{limit} values.

2) If $k > k_{limit}$, then terminate the iterations.

3) Calculate the measurement function $h(x^k)$, the measurement Jacobian $H(x^k)$, and

the gain matrix $G(x^k) = H^T(x^k)R^{-1}H(x^k)$.

4) Solve Δx^k using Equation (2.10).

5) If $\left|\Delta x^k\right| > \varepsilon$, then go to step 2). Else, stop. Algorithm converged.

2.3 Measurement and Component Modeling

There are three most commonly used measurement types in power system state estimation. They are the bus power injections, the line power flows and bus voltage magnitudes. These measurement equations can be expressed using the state variables. Consider a system having N buses, the state vector will have $(2N-1)$ components which are composed of N bus voltage magnitudes and $(N-1)$ phase angles. The state vector is equal to $x^T = [|V_1||V_2|\cdots|V_N|\theta_2\theta_3\cdots\theta_N]$. An arbitrary value, such as 0 is set to be the phase angle of one reference bus. If we define $g_{ij} + jb_{ij}$ as the admittance of the series branch line connecting buses i and j, and $g_{si} + jb_{si}$ as the admittance of the shunt branch connected at bus i, the equivalent π model can be shown in Figure 2 below.

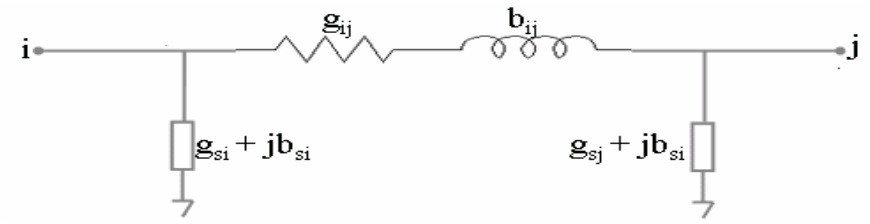

Figure 2. Equivalent 'π'Model of Two Bus System

Let the (i,j)th entry of the admittance matrix Y be $Y_{ij} = G_{ij} + jB_{ij}$. The expression for each of the above types of measurements are then given below:

Real and reactive power injection at bus i can be expressed by,

$$P_i = |V_i| \sum_{j \in N_i}^{N} |V_j| (G_{ij} \cos\theta_{ij} + B_{ij} \sin\theta_{ij}) \tag{2.11}$$

$$Q_i = |V_i| \sum_{j \in N_i}^{N} |V_j| (G_{ij} \sin\theta_{ij} - B_{ij} \cos\theta_{ij})$$

Real and reactive power flow from bus i to bus j are,

$$P_{ij} = |V_i|^2 (g_{si} + g_{ij}) - |V_i||V_j| (g_{ij} \cos\theta_{ij} + b_{ij} \sin\theta_{ij}) \tag{2.12}$$

$$Q_{ij} = -|V_i|^2 (b_{si} + b_{ij}) - |V_i||V_j| (g_{ij} \sin\theta_{ij} - b_{ij} \cos\theta_{ij})$$

Jacobian matrix H components for real power injection measurement are,

$$\frac{\partial P_i}{\partial \theta_i} = \sum_{j=1}^{N} |V_i||V_j| (-G_{ij} \sin\theta_{ij} + B_{ij} \cos\theta_{ij}) - |V_i|^2 B_{ii} \tag{2.13}$$

$$\frac{\partial P_i}{\partial \theta_j} = |V_i||V_j| (G_{ij} \sin\theta_{ij} - B_{ij} \cos\theta_{ij})$$

$$\frac{\partial P_i}{\partial |V_i|} = \sum_{j=1}^{N} |V_j| (G_{ij} \cos\theta_{ij} + B_{ij} \sin\theta_{ij}) - |V_i|^2 G_{ii}$$

$$\frac{\partial P_i}{\partial |V_j|} = |V_i| (G_{ij} \cos\theta_{ij} + B_{ij} \sin\theta_{ij})$$

Jacobian matrix H components for reactive power injection measurement are,

$$\frac{\partial Q_i}{\partial \theta_i} = \sum_{j=1}^{N} |V_i||V_j| (G_{ij} \cos\theta_{ij} + B_{ij} \sin\theta_{ij}) - |V_i|^2 G_{ii} \tag{2.14}$$

$$\frac{\partial Q_i}{\partial \theta_j} = |V_i||V_j| (-G_{ij} \sin\theta_{ij} - B_{ij} \sin\theta_{ij})$$

$$\frac{\partial Q_i}{\partial |V_i|} = \sum_{j=1}^{N} |V_j| (G_{ij} \sin\theta_{ij} - B_{ij} \cos\theta_{ij}) - |V_i|^2 B_{ii}$$

$$\frac{\partial Q_i}{\partial |V_j|} = |V_i| (G_{ij} \sin\theta_{ij} - B_{ij} \cos\theta_{ij})$$

Jacobian matrix H components for real power flow measurement are,

$$\frac{\partial P_{ij}}{\partial \theta_i} = |V_i||V_j|(g_{ij}\sin\theta_{ij} - b_{ij}\cos\theta_{ij}) \tag{2.15}$$

$$\frac{\partial P_{ij}}{\partial \theta_j} = -|V_i||V_j|(g_{ij}\sin\theta_{ij} - b_{ij}\cos\theta_{ij})$$

$$\frac{\partial P_{ij}}{\partial |V_i|} = -|V_j|(g_{ij}\cos\theta_{ij} + b_{ij}\sin\theta_{ij}) + 2(g_{ij} + g_{si})|V_i|$$

$$\frac{\partial P_{ij}}{\partial |V_j|} = -|V_i|(g_{ij}\cos\theta_{ij} + b_{ij}\sin\theta_{ij})$$

Jacobian matrix H components for reactive power flow measurement are,

$$\frac{\partial Q_{ij}}{\partial \theta_i} = -|V_i||V_j|(g_{ij}\cos\theta_{ij} + b_{ij}\sin\theta_{ij}) \tag{2.16}$$

$$\frac{\partial Q_{ij}}{\partial \theta_j} = |V_i||V_j|(g_{ij}\cos\theta_{ij} + b_{ij}\sin\theta_{ij})$$

$$\frac{\partial Q_{ij}}{\partial |V_i|} = -|V_j|(g_{ij}\sin\theta_{ij} - b_{ij}\cos\theta_{ij}) - 2(b_{ij} + b_{si})|V_i|$$

$$\frac{\partial Q_{ij}}{\partial |V_j|} = -|V_i|(g_{ij}\sin\theta_{ij} - b_{ij}\cos\theta_{ij})$$

The H matrix has rows at each measurements and columns at each variables. If the system is large, the H matrix has more zero components. Therefore, usually the sparse matrix technique is used to build this matrix.

2.4 State Estimation Algorithm with PMUs

One PMU can measure not only the voltage phasor, but also the current phasors. Figure 3 shows a 4-bus system example which has single PMU at bus 1. It has one voltage phasor measurement and three current phasor measurements, namely $V_1\angle\theta_1$, $I_1\angle\delta_1$, $I_2\angle\delta_2, I_3\angle\delta_3$.

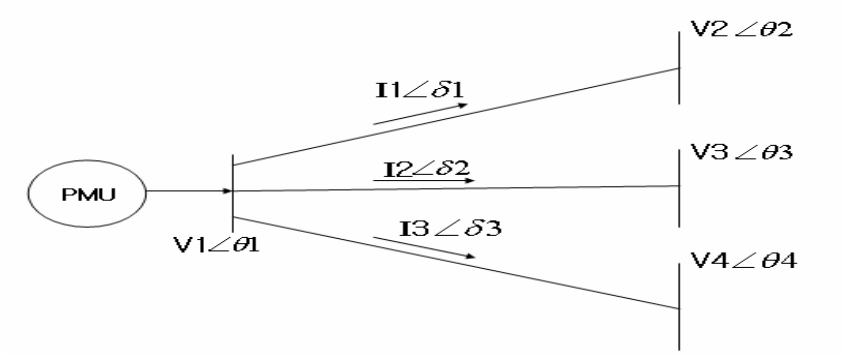

Figure 3. Single PMU Measurement Model

If we define y as the series admittance and y_{shunt} as the shunt admittance, current phasor measurements can be written in rectrangular coordinates as shown in Figure 4.

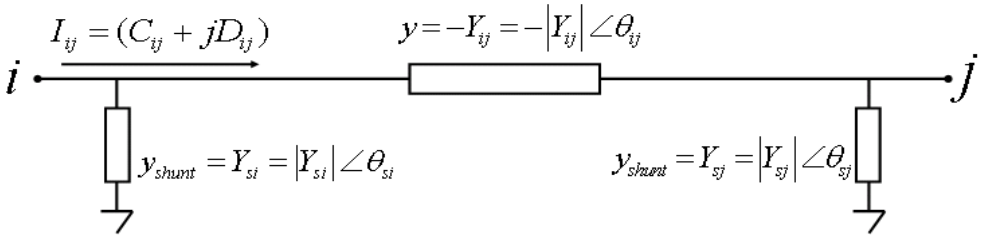

Figure 4. Transmission Line Model

The expressions for C_{ij} and D_{ij} are:

$$C_{ij} = |V_i Y_{si}|\cos(\delta_i + \theta_{si}) + |V_j Y_{ij}|\cos(\delta_j + \theta_{ij}) - |V_i Y_{ij}|\cos(\delta_i + \theta_{ij}) \qquad (2.17)$$

$$D_{ij} = |V_i Y_{si}| \sin(\delta_i + \theta_{si}) + |V_j Y_{ij}| \sin(\delta_j + \theta_{ij}) - |V_i Y_{ij}| \sin(\delta_i + \theta_{ij})$$

where, the state vector is given as : $x = [V_1 V_2 \cdots V_n \delta_2 \delta_3 \cdots \delta_n]^T$.

The entries of the measurement Jacobian H corresponding to the real and reactive parts of the current phasors are:

$$\frac{\partial C_{ij}}{\partial V_i} = |Y_{si}| \cos(\delta_i + \theta_{si}) - |Y_{ij}| \cos(\delta_i + \theta_{ij}) \tag{2.18}$$

$$\frac{\partial C_{ij}}{\partial V_j} = |Y_{ij}| \cos(\delta_j + \theta_{ij})$$

$$\frac{\partial C_{ij}}{\partial \delta_i} = -|V_i Y_{si}| \sin(\delta_i + \theta_{si}) + |V_i Y_{ij}| \sin(\delta_i + \theta_{ij})$$

$$\frac{\partial C_{ij}}{\partial \delta_j} = -|V_j Y_{ij}| \sin(\delta_j + \theta_{ij})$$

$$\frac{\partial D_{ij}}{\partial V_i} = |Y_{si}| \sin(\delta_i + \theta_{si}) - |Y_{ij}| \sin(\delta_i + \theta_{ij}) \tag{2.19}$$

$$\frac{\partial D_{ij}}{\partial V_j} = |Y_{ij}| \sin(\delta_j + \theta_{ij})$$

$$\frac{\partial D_{ij}}{\partial \delta_i} = |V_i Y_{si}| \cos(\delta_i + \theta_{si}) - |V_i Y_{ij}| \cos(\delta_i + \theta_{ij})$$

$$\frac{\partial D_{ij}}{\partial \delta_j} = |V_j Y_{ij}| \cos(\delta_j + \theta_{ij})$$

The measurement vector z contains δ, C_{ij}, D_{ij}, as well as the power injections, power flows and voltage magnitude measurements.

$$z = [P_{inj}{}^T, Q_{inj}{}^T, P_{flow}{}^T, Q_{flow}{}^T, |V|^T, \delta^T, C_{ij}{}^T, D_{ij}{}^T]^T \tag{2.20}$$

Generally, those measurements received from PMUs are more accurate with small variances compared to the variances of conventional measurements. Therefore, including PMU measurements is expected to produce more accurate estimates. Multi-area state estimation also benefits from this technology.

2.5 Observability and Bad Data Detection

If the entire state vector of bus voltage magnitudes and angles can be estimated from the set of available measurements, the power system with the specified measurement set is said to be observable. However, some measurement failures may occur in the power system at anytime. In this situation, the power system state estimator can not estimate bus voltage magnitudes and angles at all buses. It can only estimate a portion of the entire network. If a limited number of measurement units are exist, then the units should be placed properly to make the entire system observable. Observability and measurement placement problems are well described in [24]-[27]. Other than these problems, the method of bad data detection is also studied in this thesis.

Every actual measurement may contain small random errors due to various reasons, such as the limited precision of the measuring meters and the unexpected noise in the communication channals. However, such errors may be filtered out by the state estimator. One of the essential functions of a state esimator is to detect gross measurement errors, and to identify and eliminate them if possible. Different kinds of bad data processing methods are explained in [28]-[32].

When using the WLS estimation method, detection and identification of bad data are done only after the estimation algorithm converges, by processing the measurement residuals. In this thesis, chi-squares detection test and largest normalized residual test will be discussed. The chi-squares test only determines if the measurement set has any bad data. Once bad data are detected, they need to be identified and eliminated or corrected. The largest normalized residual has the ability to identify bad data.

Consider the objective function $J(x)$, written in terms of the measurement errors,

$$J(x) = \sum_{i=1}^{m} R_{ii}^{-1} e_i^2 = \sum_{i=1}^{m} \left(\frac{e_i}{\sqrt{R_{ii}}}\right)^2 = \sum_{i=1}^{m} (e_i^N)^2 \qquad (2.21)$$

e_i is the ith measurement error, R_{ii} is the diagonal entry of the measurement error covariance matrix and m is the total number of measurements. Assuming that e_i's are all normally distributed random variables with zero mean and R_{ii} variances, e_i^N's will have a

standard normal distribution, i.e.:

$$e_i^N \sim N(0,1) \tag{2.22}$$

Then, $J(x)$ will have a χ^2 distribution with at most $(m-n)$ degree of freedom. $\chi^2_{(m-n),\alpha}$ means chi-squares distribution with $(m-n)$ degrees of freedom with probability of false alarm α. $J(x)$ value which is larger than the distribution curve $\chi^2_{(m-n),\alpha}$ indicates that there are bad data in the measurement set. After detecting bad data, identification and elimination of bad data is required.

Considering the residual sensitivity and covariance matrices, measurement residuals may still be correlated even if errors are assumed independent with $E(e)=0$, $\text{cov}(e)=R$. Then, the WLS estimator of the linearized state vector will be given by,

$$\Delta\hat{x} = (H^T R^{-1} H)^{-1} H^T R^{-1} \Delta z \ = G^{-1} H^T R^{-1} \Delta z \tag{2.23}$$

If we define K matrix which is sometimes called the hat matrix as $K = HG^{-1}H^T R^{-1}$, then the estimated value of Δz can be denoted by:

$$\Delta\hat{z} = H\Delta\hat{x} = K\Delta z \tag{2.24}$$

Now, the measurement residuals can be expressed as follows:

$$\begin{aligned} r = \Delta z - \Delta\hat{z} &= (I-K)\Delta z \\ &= (I-K)(H\Delta x + e) = (I-K)e \\ &= Se \end{aligned} \tag{2.25}$$

The matrix S, called the residual sensitivity matrix, represents the sensitivity of the measurement residuals to the measurement errors. Normalized value of the residual for measurement i can be obtained by simply dividing its absolute value by the corresponding diagonal entry in the residual covariance matrix,

$$r_i^N = \frac{|r_i|}{\sqrt{\Omega_{ii}}} = \frac{|r_i|}{\sqrt{R_{ii}S_{ii}}} \tag{2.26}$$

The normalized residual vector r^N will then have a standard normal distribution, i.e. $r_i^N \sim N(0,1)$. Thus, the largest element in r^N can be compared against a statistical threshold to decide on the existence of bad data. This threshold can be chosen based on the

desired level of detection sensitivity.

Bad data may show up in several different ways depending on the type, location and number of measurements that are in error. When there are multiple bad data in the measurement set, estimates of measuerments may be significantly affected by the errors of each other, if they have strongly correlated residuals. They are referred to as interacting bad data which will make bad data processing very difficult. Futhurmore, conforming errors are those that appear consistent with each other, making their identification more difficult.

When a single bad measurement exists in the measurement set, the largest normalized residual test will identify and eliminate the bad data, but only if the measurement is not critical. A critical measurement is the one whose elimination from the measurement set will result in an unobservable system. The measurement residual of a critical measurement will always be zero. There are also critical pairs and critical k-tuples. When simultaneous removal of two redundant measurements makes the system unobservable, it is called a critical pair. A critical k-tuple contains k redundant measurements, where removal of all of them will cause the system to become unobservable. Therefore, the bad data processing is not so easy when there are multiple interacting or conforming bad data or any critical measurements which are bad.

CHAPTER III
LINEAR FORMULATION OF STATE ESTIMATION USING ONLY PMUS

3.1 Introduction

One phasor measurement unit can measure a synchronized voltage phasor and several synchronized current phasors. If the measurement set is composed of only voltages and currents measured by PMUs, the state estimation can be formulated as a linear problem. The state vector and measurement data can be expressed in rectrangular coordinate system. The voltage measurement ($V = |V| \angle \theta$) can be expressed as ($V = E + jF$), and the current measurement can be expressed as ($I = C + jD$).

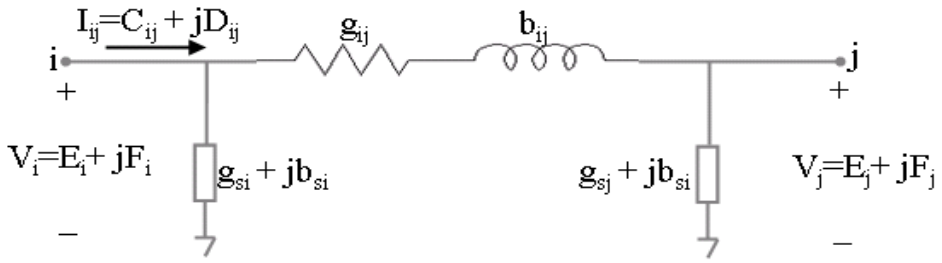

Figure 5. Transmission Line Model with Rectangular Form

In the Figure 5, ($g_{ij} + jb_{ij}$) is the series admittance of the line, and ($g_{si} + jb_{si}$) is the shunt admittance of the transmission line. Line current flow I_{ij} can be expressed as a linear fucntion of voltages.

$$\begin{aligned} I_{ij} &= [(V_i - V_j) \times (g_{ij} + jb_{ij})] + [V_i \times (g_{si} + jb_{si})] \\ &= [(g_{ij} + jb_{ij}) + (g_{si} + jb_{si})] \times V_i - (g_{ij} + jb_{ij}) \times V_j \end{aligned} \tag{3.1}$$

The measurement vector z is expressed as $z = h(x) + e$, (where x is a state vector, $h(x)$ is a matrix of the linear equations, and e is an error vector). In rectangular coordinates:

$$z = (Hr + jHm)(E + jF) + e \tag{3.2}$$

where, $H = Hr + jHm$, $x = E + jF$ and $z = A + jB$.

A and B are expressed by:

$$A = Hr \times E - Hm \times F \tag{3.3}$$
$$B = Hm \times E + Hr \times F$$

In matrix form,

$$\begin{bmatrix} A \\ B \end{bmatrix} = \begin{bmatrix} Hr & -Hm \\ Hm & Hr \end{bmatrix} \begin{bmatrix} E \\ F \end{bmatrix} + e \tag{3.4}$$

Then, the estimated value $\hat{x} = \hat{E} + j\hat{F}$ can be obtained by solving the linear equation below:

$$\hat{x} = (H^T R^{-1} H)^{-1} H^T R^{-1} z \tag{3.5}$$

If we define the linear matrix H_{new} as $H_{new} = \begin{bmatrix} Hr & -Hm \\ Hm & Hr \end{bmatrix}$, then the above equation can be rewritten by:

$$\hat{x} = \begin{bmatrix} \hat{E} \\ \hat{F} \end{bmatrix} = (H_{new}{}^T R^{-1} H_{new})^{-1} H_{new}{}^T R^{-1} \begin{bmatrix} A \\ B \end{bmatrix} \tag{3.6}$$

Therefore, the equation for rectangular formed variable $\hat{x}$ can be given by the rectangular forms of H matrix and z vector. They are all real numbers.

3.2 Linear State Estimation Algorithm

Consider the two bus system shown in Figure 6. Note that PMU located at bus 1 measures voltage V_1 and line current I_{12}. According to (3.1), the line current flow I_{12} can be expressed as:

$$I_{12} = k_1 \times V_1 + k_2 \times V_2 \quad (k_1, k_2 \text{ are constant complex value}) \tag{3.7}$$

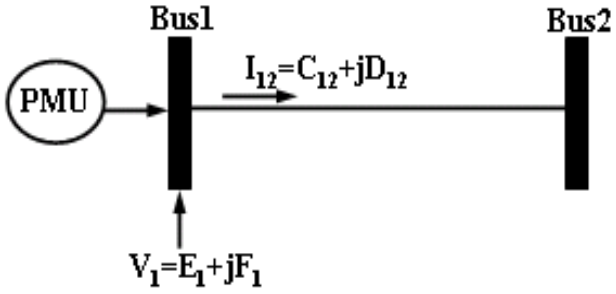

Figure 6. Two Bus System with Measurements

Measurement vector z has two entries, V_1 and I_{12}.

$$z = \begin{bmatrix} V_1 \\ I_{12} \end{bmatrix} = \begin{bmatrix} 1 & 0 \\ k_1 & k_2 \end{bmatrix} \begin{bmatrix} E \\ F \end{bmatrix} + e \tag{3.8}$$

Expressing (3.8) in rectrangular coordinates:

$$\begin{bmatrix} 1 & 0 \\ k_1 & k_2 \end{bmatrix} = \begin{bmatrix} 1 & 0 \\ kr_1 + jkm_1 & kr_2 + jkm_2 \end{bmatrix} = \begin{bmatrix} 1 & 0 \\ kr_1 & kr_2 \end{bmatrix} + j \begin{bmatrix} 0 & 0 \\ km_1 & km_2 \end{bmatrix} = Hr + jHm$$

where, $V_1 = E_1 + jF_1$, $\quad I_{12} = C_{12} + jD_{12}$

$k_1 = kr_1 + jkm_1$, $\quad k_2 = kr_2 + jkm_2$

The measurement vector z becomes,

$$z = \begin{bmatrix} E_1 \\ C_{12} \\ F_1 \\ D_{12} \end{bmatrix} = \begin{bmatrix} 1 & 0 & 0 & 0 \\ kr_1 & kr_2 & -km_1 & -km_2 \\ 0 & 0 & 1 & 0 \\ km_1 & km_2 & kr_1 & kr_2 \end{bmatrix} \begin{bmatrix} E_1 \\ E_2 \\ F_1 \\ F_2 \end{bmatrix} + e \tag{3.9}$$

Finally, $\hat{x}$ is calculated using (3.6):

$$\hat{x} = \begin{bmatrix} \hat{E} \\ \hat{F} \end{bmatrix} = \begin{bmatrix} E_1 \\ E_2 \\ F_1 \\ F_2 \end{bmatrix}, \quad z = \begin{bmatrix} A \\ B \end{bmatrix} = \begin{bmatrix} E_1 \\ C_{12} \\ F_1 \\ D_{12} \end{bmatrix} \tag{3.10}$$

This is very simple and fast, because it dosen't need any iterations.

3.3 Simulation Results

Four different IEEE test systems (IEEE14, IEEE30, IEEE57, IEEE118 bus system) are used for the simulations [33]-[35]. A gaussian random errors are imposed on each measurement. The error variance of measurements is set to be 0.00001. Table 1 shows the locations of PMUs at each system. These PMUs are placed as a minimum required number. Each PMU has one voltage measurement and several current flow measurements connected to the neighboring buses.

Table 1. PMU Locations for Each IEEE System

	PMU locations at Bus
IEEE14 Bus	2,6,7,9
IEEE30 Bus	3,5,6,9,10,12,19,23,25,29
IEEE57 Bus	1,4,7,9,15,20,24,25,27,32,36,38,39,41,46,50,53
IEEE118 Bus	2,5,9,11,12,17,21,24,25,28,34,37,40,45,49,52,56, 62,63,68,73,75,77,80,85,86,90,94,101,105,110,114

Network diagrams showing the PMU locations for the test systems are given in Figures 7~10.

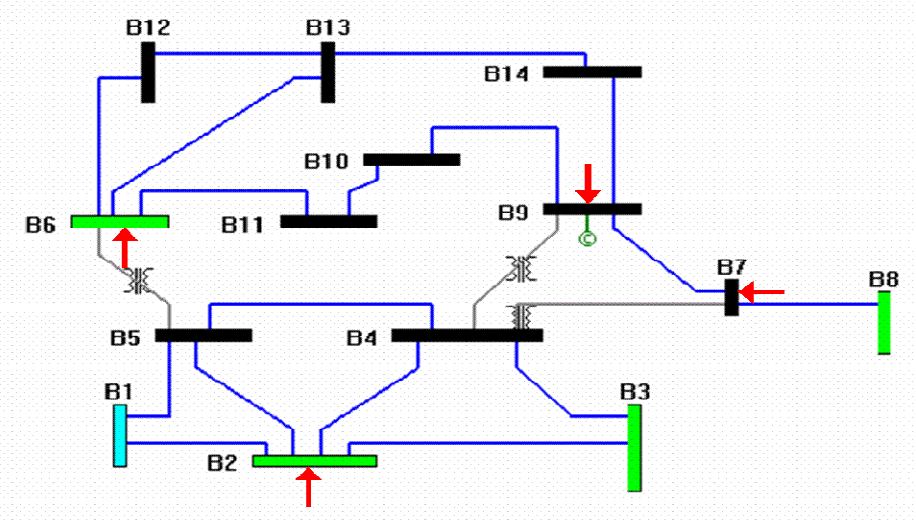

Figure 7. IEEE14 Bus System with PMU Locations

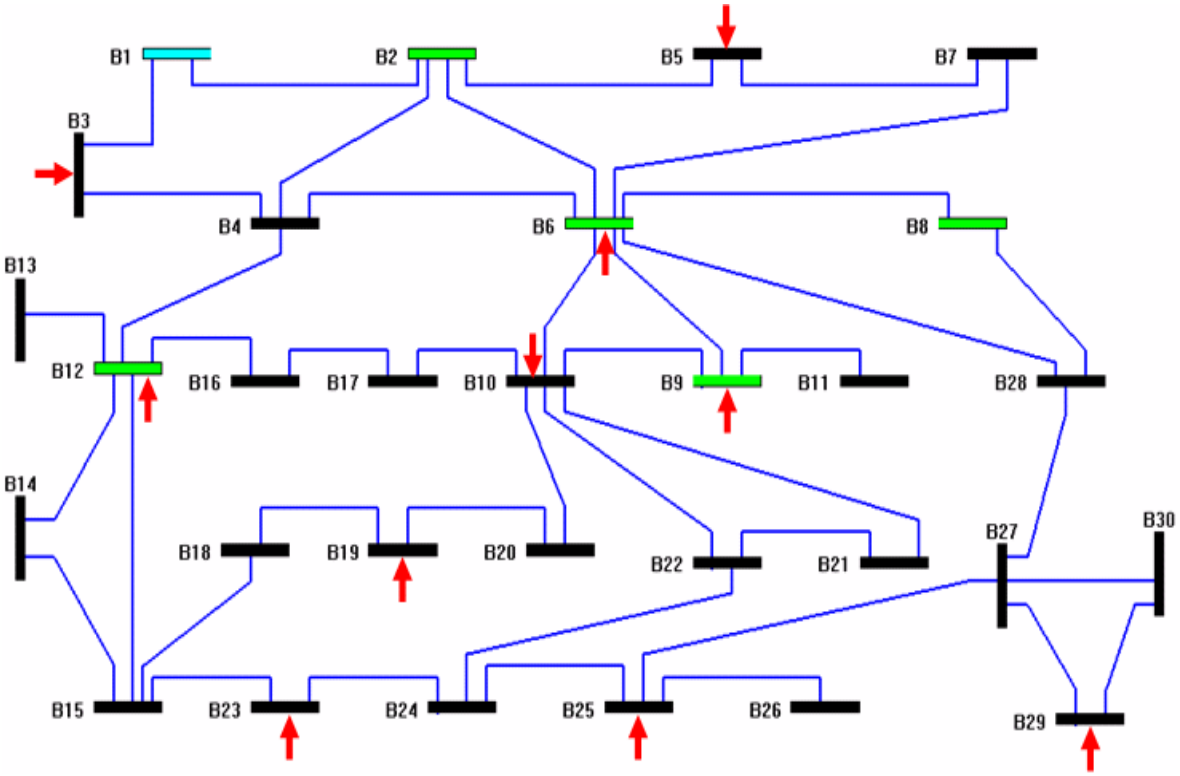

Figure 8. IEEE30 Bus System with PMU Locations

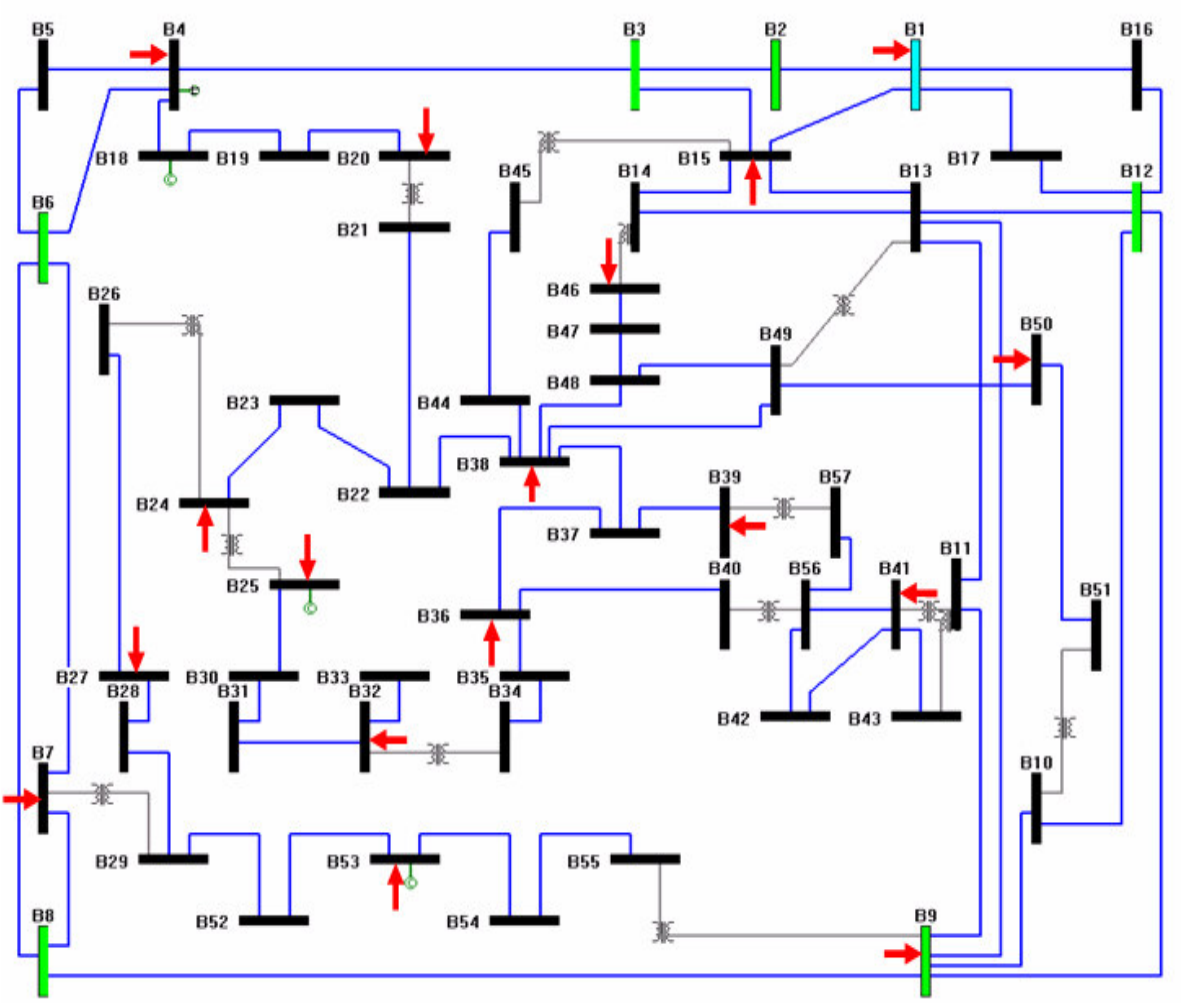

Figure 9. IEEE57 Bus System with PMU Locations

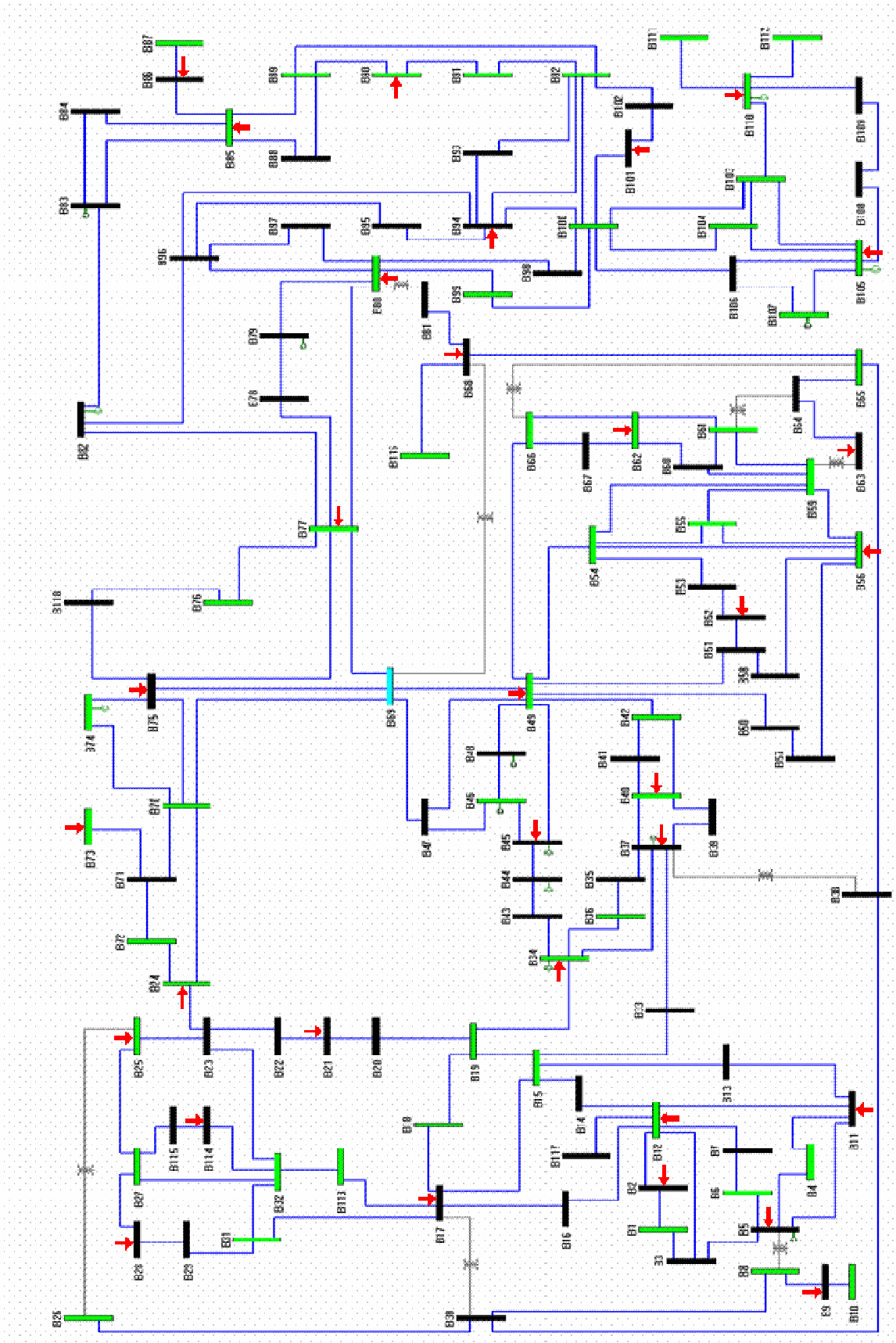

Figure 10. IEEE118 Bus System with PMU Locations

Table 2 shows the total results of the state estimation using only PMUs. The objective functions $J(x)$ is also much less than the chi-squares threshold with 99% confidence.

Table 2. Linear Formulation Simulation Results of Several IEEE Bus Systems

	IEEE 14Bus	IEEE 30Bus	IEEE 57Bus	IEEE 118Bus
Number of PMUs	4	10	17	32
Number of voltage measure	4	10	17	32
Number of current measure	15	34	54	125
H matrix dimension	38 by 27	88 by 59	142 by 113	314 by 235
Computation time (s)	0.11	0.161	0.341	0.451
Degree of freedeom	11	29	29	79
Chi-square limit	24.725	49.588	49.588	111.144
J(x) (objective function)	0.0678	0.0938	0.0877	0.3538
Largest normalized residual	0.2275	0.1485	0.1586	0.2293

3.4 Bad Data Processing

The method of bad data detection and identification with linear formulation of state estimation is investigated in this section. Bad data processing includes chi-squares test and largest normalized residual test. As an example, Figure 11 shows a portion of the IEEE118 bus system with PMU locations at bus 37 and bus 40.

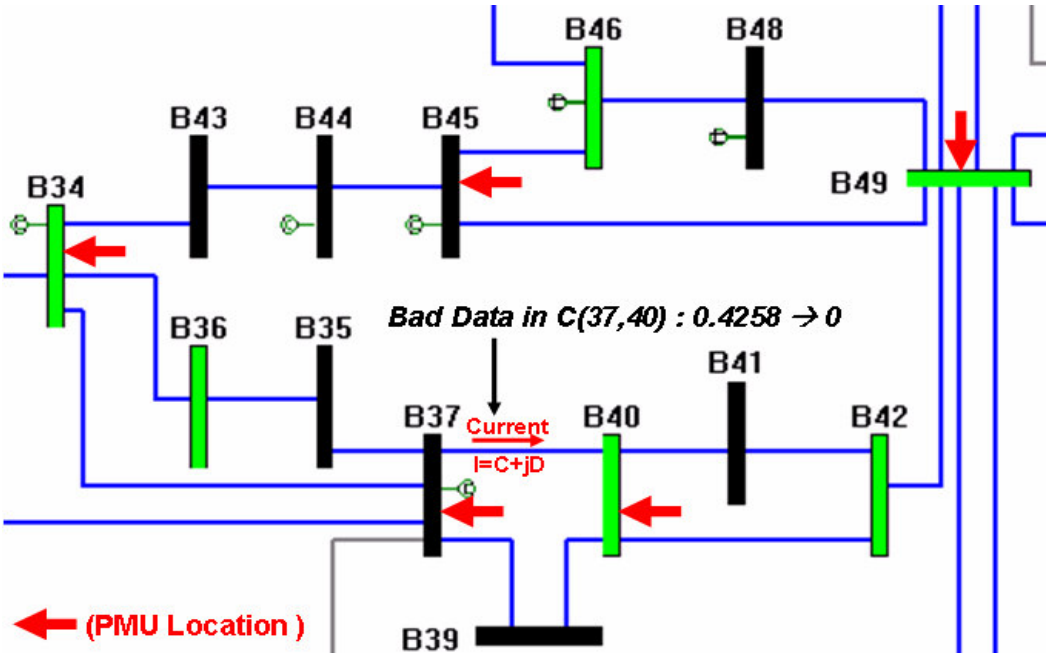

Figure 11. Imposed Bad Data at C(37,40) from 0.4258 to 0 in IEEE118 Bus System

One bad data is imposed to the current measurement from bus 37 to bus 40. Real part of current measurement (37,40) is 0.4258 in normal operating condition. C(37,40) is forced to change from 0.4258 to 0. There are PMUs in bus 37 and 40. Therefore, C(37,40) is a redundant measurement. The state estimation result with objective function is shown in Table 3. The objective function J(x) is much larger than chi-sqaures limit, which means that the test detected bad data. Then, the largest normalized residual test identified the bad data at C(37,40) which has the largest normalzied residual of 369.72 in Table 4.

Table 3. Objective Function Value with Bad Data at C(37,40)

Degree of Freedom	Chi-Sqaures limit	Objective function J(x)
78	109.96	13595

Table 4. Sorted Normalized Residual Test Results with Bad Data

Measurement Type	Sorted Normalized Residual
Real part of current measurement (37,40)	369.72
Real part of current measurement (40,39)	207.37
Real part of current measurement (37,39)	207.35
Real part of current measurement (40,37)	122.37
:	:

The current measurement (37,40) has been removed, because the real part of current measurement has been identified as a bad data. After removing it, the chi-squares test did not detect any bad data, and the largest normalized residual is 0.21842 which is far below the test criteria 3.0, as shown in Tables 5-6.

Table 5. Objective Function Value with No Bad Data

Degree of Freedom	Chi-sqaures limit	Objective function J(x)
76	107.58	0.3612

Table 6. Sorted Normalized Residual Test Results with No Bad Data

Measurement Type	Sorted Normalized Residual
Real part of current measurement (85,86)	0.21842
Real part of current measurement (86,85)	0.21683
Real part of current measurement (77,75)	0.20642
Real part of voltage measurement (11)	0.20138
:	:

In this example, the bad data C(37,40) has been successfully detected and sorted out with two tests, a chi-squares test and a largest normalized residual test.

CHAPTER IV
BENEFITS OF USING PMUS

4.1 Improved Accuracy of Variables with PMUs

This section investigates the effects of increasing the number of PMUs on the accuracy of the estimated variables. If some PMU measurements are added to the state estimation, the state estimation accuracy will be affected, because the PMU measurements have smaller error variances compared to other measurements. One PMU has one voltage phasor measurement and several current phasor measurements at any branch connected to the PMU installed bus. A PMU will measure two quantities, the real and reactive part of the phasor for each voltage or current.

Firstly, consider how to measure the accuracy of the estimated variables. One of the way of representing the level of state estimation accuracy is to refer the covariance of the estimated variables. From (3.5), the covariance of the estimated variable vector $\hat{x}$ can be expressed as:

$$Cov(\hat{x}) = Cov((H^T R^{-1} H)^{-1} H^T R^{-1} z) = Cov(G^{-1} H^T R^{-1} z) \tag{4.1}$$

The covariance of the measurement vector z is R from (2.4):

$$Cov(z) = Cov(h(x) + e) = Cov(e) = R \tag{4.2}$$

Then, (4.1) can be rewritten as:

$$\begin{aligned} Cov(\hat{x}) &= (G^{-1} H^T R^{-1}) Cov(z) (G^{-1} H^T R^{-1})^T \\ &= (G^{-1} H^T R^{-1}) R ((H^T R^{-1} H)^{-1} H^T R^{-1})^T \\ &= (G^{-1} H^T R^{-1}) R (H^T R^{-1})^T ((H^T R^{-1} H)^{-1})^T \\ &= (G^{-1} H^T R^{-1}) R R^{-1} H H^{-1} R (H^T)^{-1} \\ &= G^{-1} H^T R^{-1} R (H^T)^{-1} \\ &= G^{-1} \end{aligned} \tag{4.3}$$

Therefore, the inverse of the gain matrix is equal to the covariance of the $\hat{x}$.

Consider a three bus system example of Figure 12. All the line impedances are assumed to be ‘j10’. There are 5 measurements shown in Table 7. S.D. means an error

standard deviation.

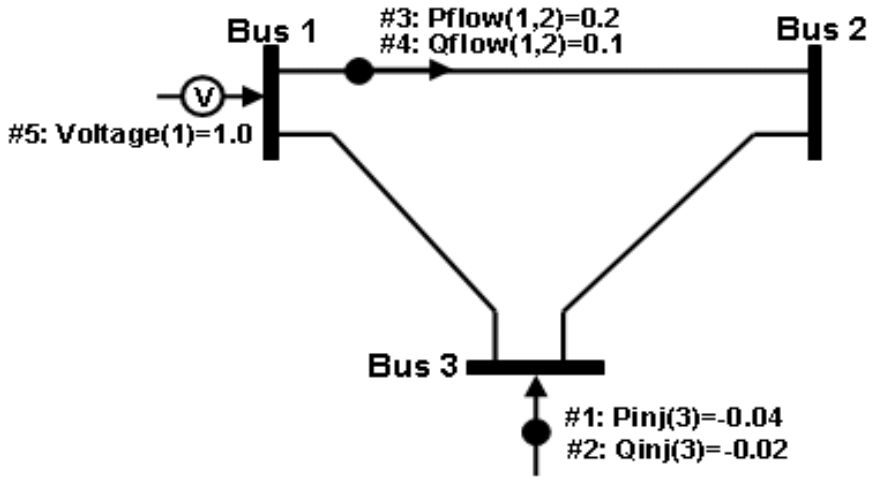

Figure 12. Three Bus System with Measurement Data

Table 7. Measurement Type, Value and Error Standard Deviation

Measure	#1: Pflow(1,2)	#2: Qflow(1,2)	#3: Pinj(3)	#4: Qinj(3)	#5: Voltage(1)
Value	0.2	0.4	-0.04	-0.02	1.0
S.D.	0.01	0.01	0.01	0.01	0.004

Variable vector x in the system can be express as $x = [|V_i|^T, \delta_i^T]$.

With 3-bus example, $|V_i|^T = [|V_1|, |V_2|, |V_3|]$, $\delta_i^T = [\delta_2, \delta_3]$ (bus 1 is chosen as slack).

The Jacobian matrix, 'H' and the inverse of weight, 'R' can be calculated as:

$$H=\begin{bmatrix} -39.8 & 40 & 0 & 0.1 & 0 \\ 0.1 & 0.1 & 0 & -40.2 & 0 \\ 40.12 & 40.12 & -80.28 & 0.04 & 0.02 \\ -0.06 & 0.04 & -0.02 & -40.32 & 80.44 \\ 1 & 0 & 0 & 0 & 0 \end{bmatrix}, R=\begin{bmatrix} 0.0001 & 0 & 0 & 0 & 0 \\ 0 & 0.0001 & 0 & 0 & 0 \\ 0 & 0 & 0.0001 & 0 & 0 \\ 0 & 0 & 0 & 0.0001 & 0 \\ 0 & 0 & 0 & 0 & 0.000016 \end{bmatrix}$$

Inverse of gain matrix can be calculated by (2.8), $G^{-1}=\left(H^{T}R^{-1}H\right)^{-1}$:

$$G^{-1}=\begin{bmatrix} 1.6\times10^{-5} & 1.592\times10^{-5} & 1.5952\times10^{-5} & 7.9205\times10^{-8} & 4.7713\times10^{-8} \\ 1.592\times10^{-5} & 1.5903\times10^{-5} & 1.5903\times10^{-5} & 7.8809\times10^{-8} & 4.7451\times10^{-8} \\ 1.5952\times10^{-5} & 1.5903\times10^{-5} & 1.5935\times10^{-5} & 7.9007\times10^{-8} & 4.7586\times10^{-8} \\ 7.9205\times10^{-8} & 7.8809\times10^{-8} & 7.9007\times10^{-8} & 6.2271\times10^{-8} & 3.1253\times10^{-8} \\ 4.7713\times10^{-8} & 4.7451\times10^{-8} & 4.7586\times10^{-8} & 3.1253\times10^{-8} & 3.1144\times10^{-8} \end{bmatrix}$$

If we have the value of the inverse of the gain matrix 'G^{-1}', we can find error variances of variables by taking diagonal elements.

$$G^{-1}=\mathrm{cov}(\hat{x})\ ,\ \sqrt{G^{-1}{}_{ii}}=\sigma_{\hat{x}} \tag{4.4}$$

$$\text{Error Variance } (\sigma^2) \text{ is } G^{-1}{}_{ii}(diagonal)=\begin{bmatrix} 1.6\times10^{-5} \\ 1.5903\times10^{-5} \\ 1.5935\times10^{-5} \\ 6.2271\times10^{-8} \\ 3.1144\times10^{-8} \end{bmatrix}$$

Table 8. Variances and Standard Deviations of the Variables of Three Bus System

Measure	$\lvert V_1\rvert$	$\lvert V_2\rvert$	$\lvert V_3\rvert$	δ_2	δ_3
Variance ($\sigma_{\hat{x}}{}^2$)	1.6×10^{-5}	1.5903×10^{-5}	1.5935×10^{-5}	6.2271×10^{-8}	3.1144×10^{-8}
S.D. ($\sigma_{\hat{x}}$)	0.004	0.0039878	0.0039919	0.00024954	0.00017648

In Table 8, the error standard deviation of variable $|V_1|$ is obtained as 0.004 from the square root of the first element of the inverse gain matrix, $|V_2|$ as 0.0039878, and so on.

Regarding the accuracy, PMU can deliver more precise measurement data. Several cases are tested with different number of added PMUs to the conventional measurement set . Simulations and analysis of six different cases which are shown in Table 9 are done with several IEEE bus systems in the next section.

Table 9. Six Different Cases by Adding PMUs

Case 1	Conventional Measurements with No PMUs
Case 2	Conventional Measurements with PMUs of (10% of bus number)
Case 3	Conventional Measurements with PMUs of (20% of bus number)
Case 4	Conventional Measurements with PMUs of (30% of bus number)
Case 5	Conventional Measurements with PMUs of (40% of bus number)
Case 6	Only Minimum PMUs

4.2 Simulations Results

In this section, 4 different IEEE bus systems (IEEE14 bus system, IEEE30 bus system, IEEE57bus system, IEEE118bus system) are tested with 6 cases to find out the effect of the PMUs to the accuracy of the estimated variables.

Define m as the number of measurements, n as the number of variables, and η as the ratio of the number of measurements per the number of variables. During the tests, η is maintained to be 1.6. Table 10 has more detailed information about the measurement numbers for the tests.

Table 10. Variable Numbers and Measurement Type and Numbers

	Variables	Measurements				Ratio η $(\frac{m}{n})$
		Power Injection	Power Flow	Voltage Magnitude	Total	
IEEE14 Bus	27	18	24	1	43	1.6
IEEE30 Bus	59	38	56	1	95	1.6
IEEE57 Bus	113	72	108	1	181	1.6
IEEE118 Bus	235	150	226	1	376	1.6

For 14 bus system example, variable number is $n = 14 \times 2 - 1 = 27$ (excluding slack bus angle), and m should be 43 to maintain $\eta = 1.6$. To place measurement evenly at each system, 40% of injection easurements and 60% of flow measurements are distributed to each systems. Therefore, the injection measurement number is 18 and flow measurement number is 24 in 14 bus system. Lastly one voltage magnitude measurement is placed at each system. The settings for error standard deviations for those measurements are shown in Table 11. A PMU has much smaller error deviations than other conventinal measurements as 0.00001.

Table 11. Standard Deviations of the Measurements for the Test

Power Injection	Power Flow	Voltage Magnitude	PMU
0.01	0.008	0.004	0.00001

Figures 13~16 show the network diagrams for each systems. Arrow with circle at the bus means a pair of real and reactive power injection measurements, and arrow with ‘v’

means a voltage magnitude measurement. If there's any point on the transmission line, it means a pair of real and reactive power flow measurements. The point is placed at the starting position regarding the direction of the flow measurement.

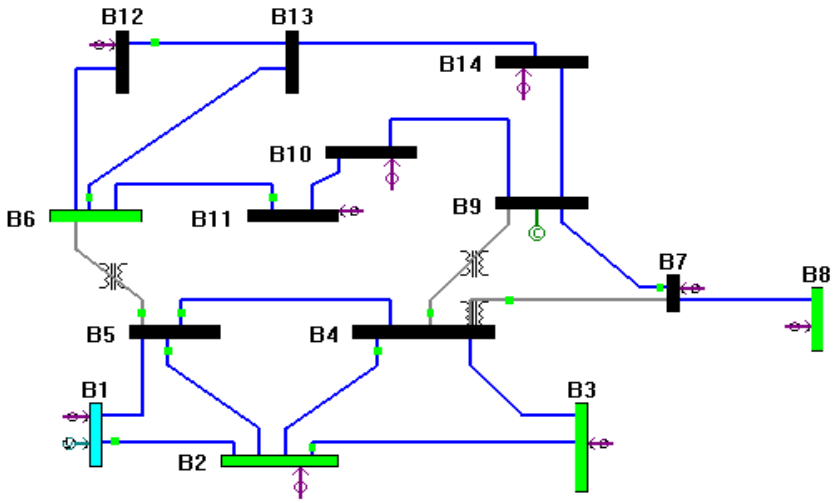

Figure 13. IEEE14 Bus System Diagram with Conventional Measurements

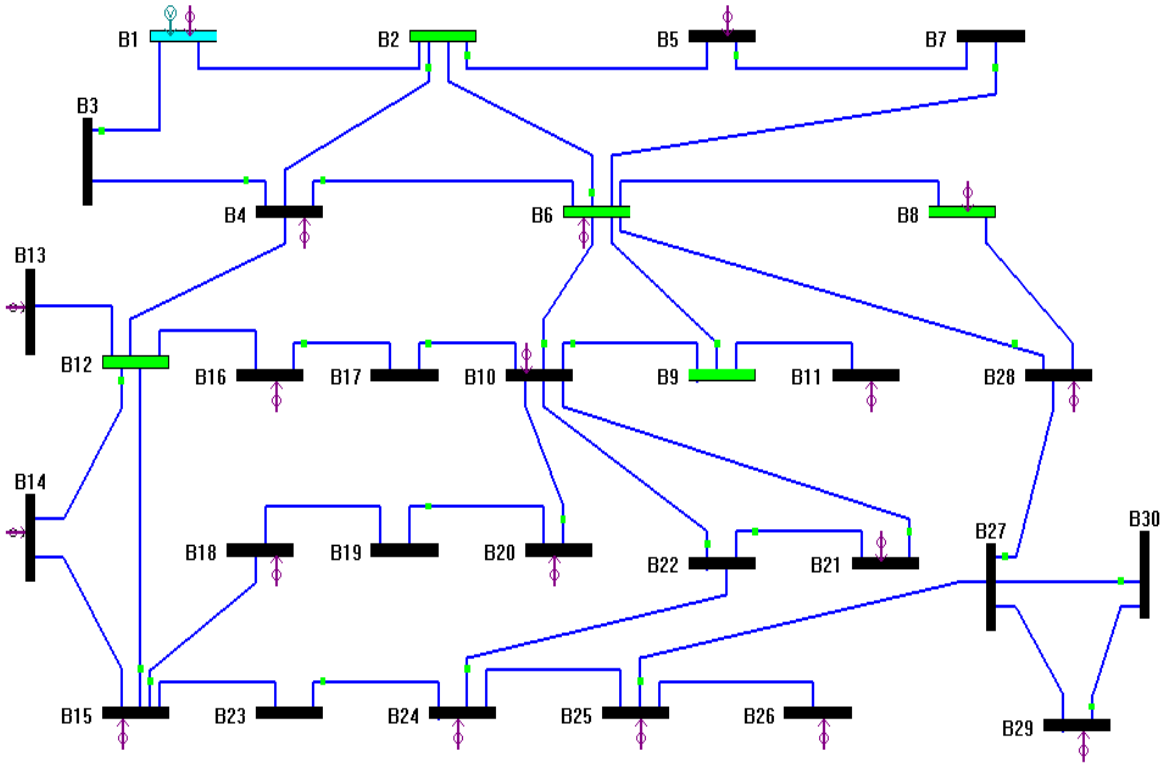

Figure 14. IEEE30 Bus System Diagram with Conventional Measurements

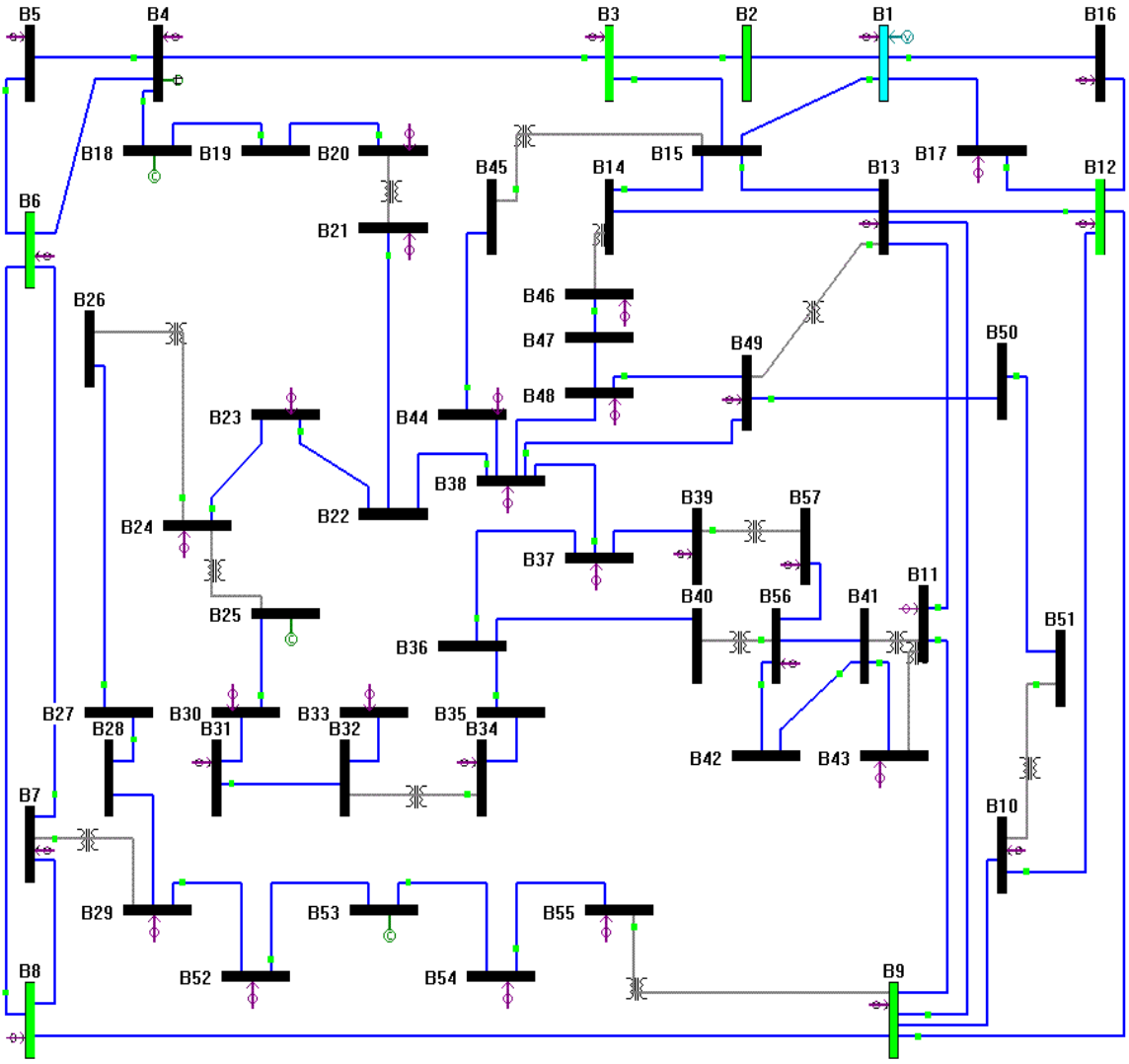

Figure 15. IEEE57 Bus System Diagram with Conventional Measurements

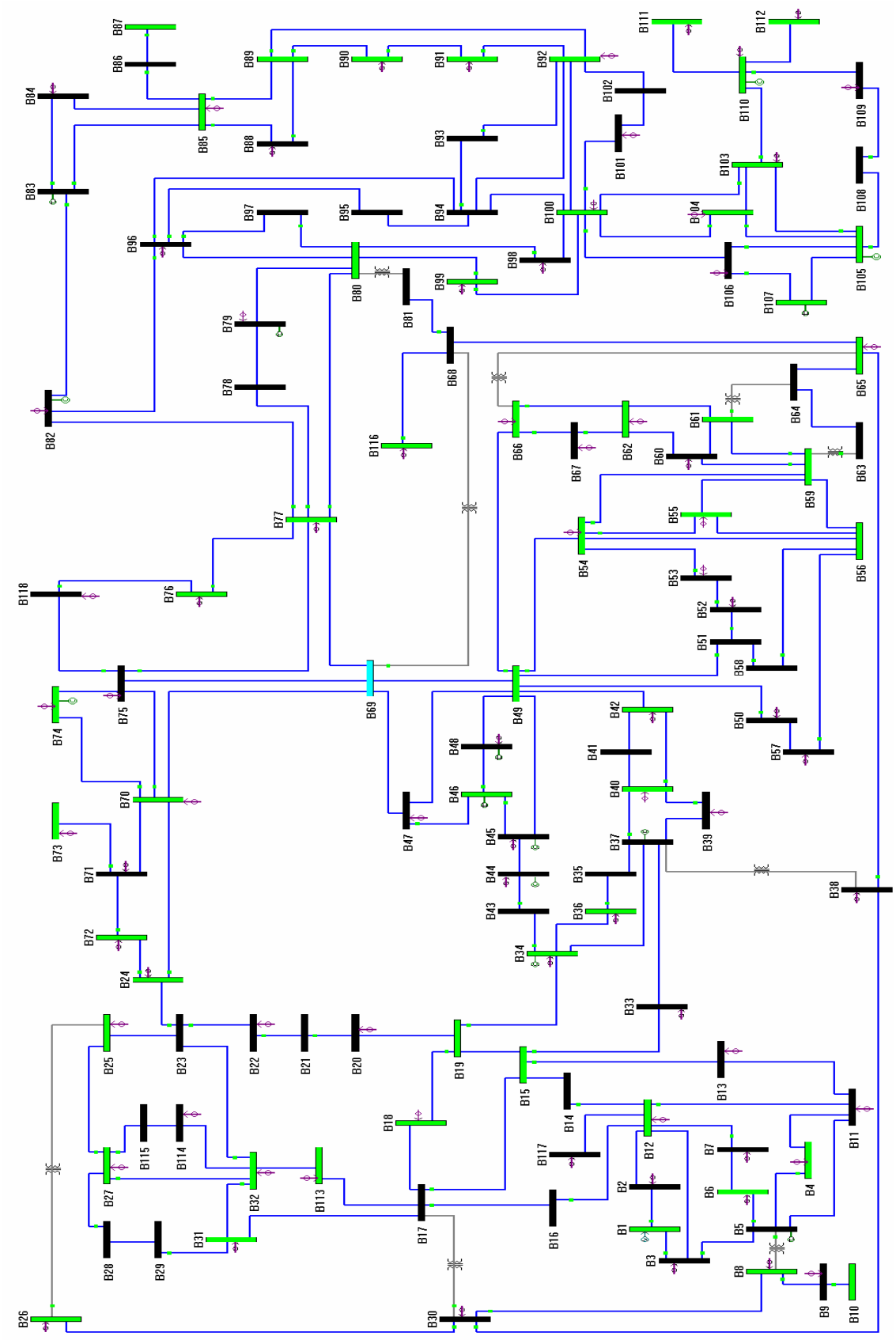

Figure 16. IEEE118 Bus System Diagram with Conventional Measurements

The accuracy of two variables (voltage magnitude, voltage angle) are investigated separately. The variances of variables are obtained from the inverse diagonal elements of 'G' matrix. The standard deviation is a square root of the variance. Figures 17~20 show the accuracy of the estimated voltage magnitudes of each system, and Figures 21~24 show the accuracy of the estimated voltage angles of each system.

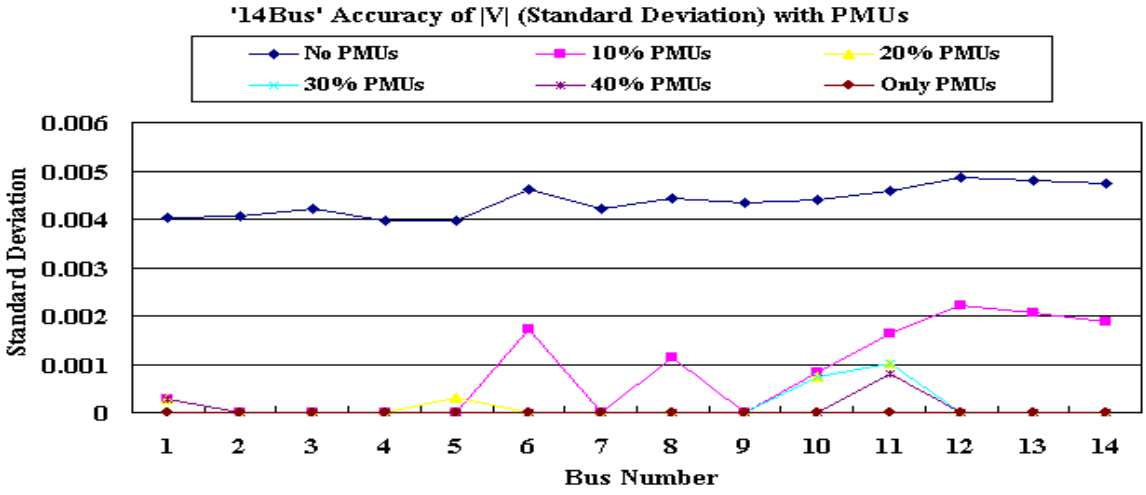

Figure 17. Accuracy of |V| of IEEE14 Bus System with PMUs

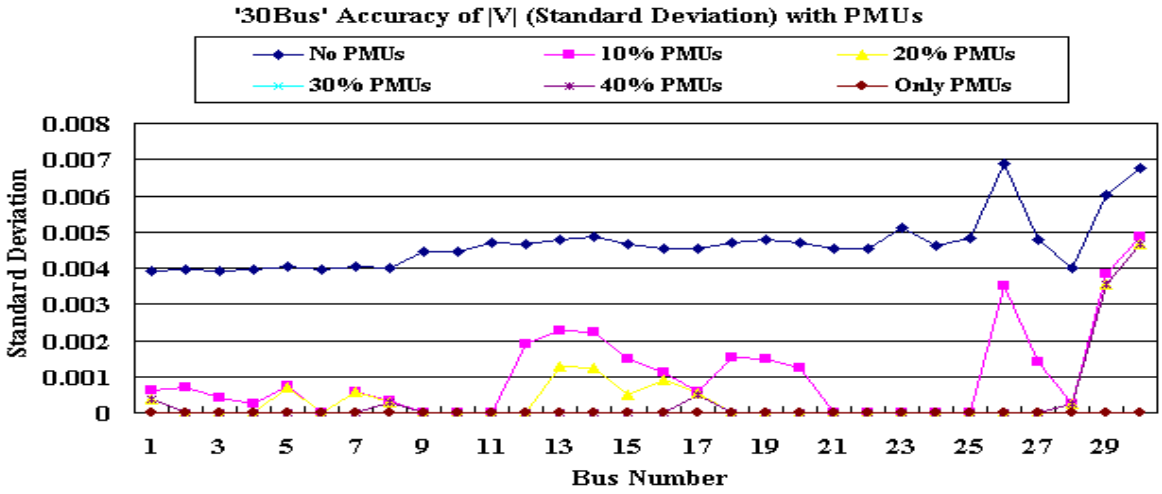

Figure 18. Accuracy of |V| of IEEE30 Bus System with PMUs

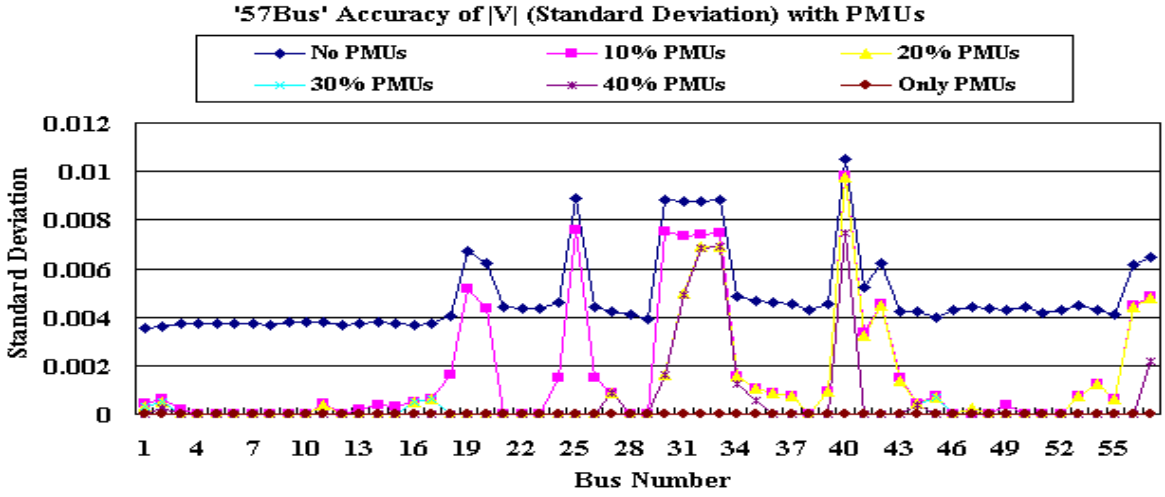

Figure 19. Accuracy of |V| of IEEE57 Bus System with PMUs

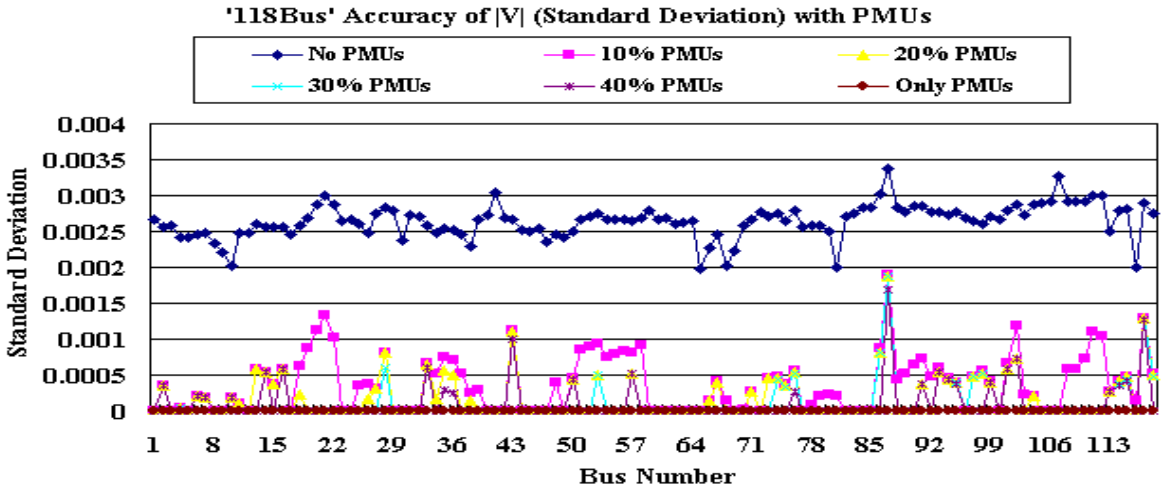

Figure 20. Accuracy of |V| of IEEE118 Bus System with PMUs

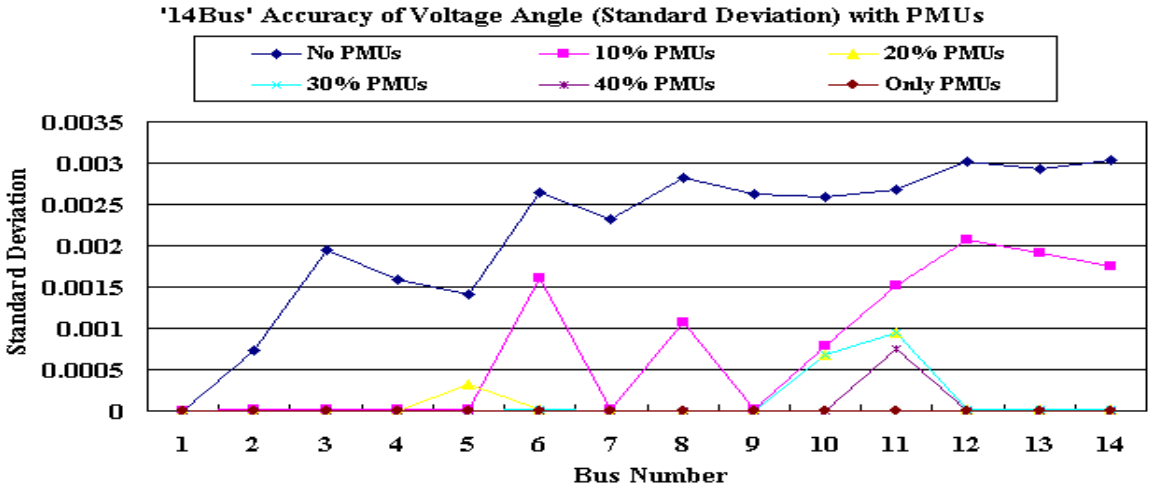

Figure 21. Voltage Angle Accuracy of IEEE14 Bus System with PMUs

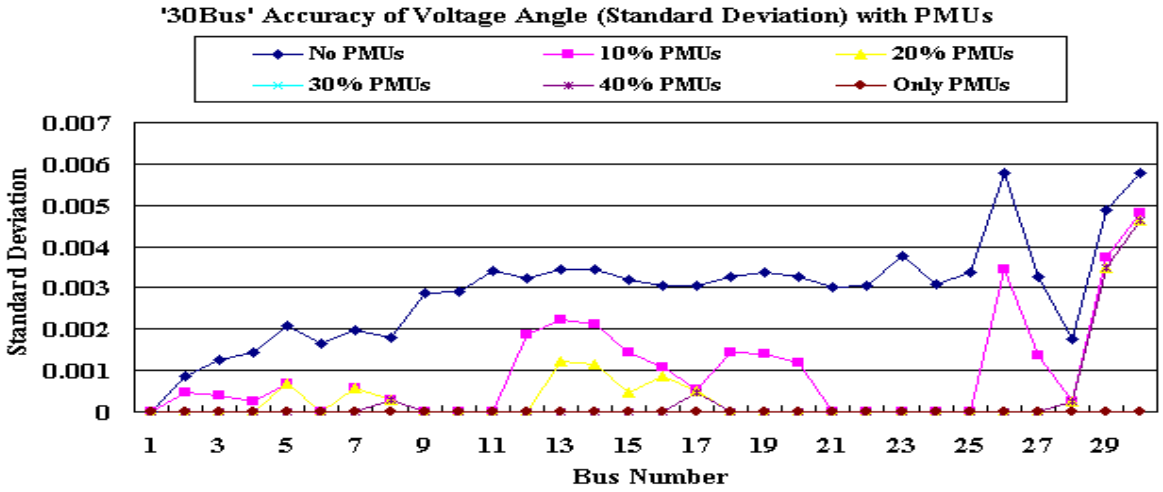

Figure 22. Voltage Angle Accuracy of IEEE30 Bus System with PMUs

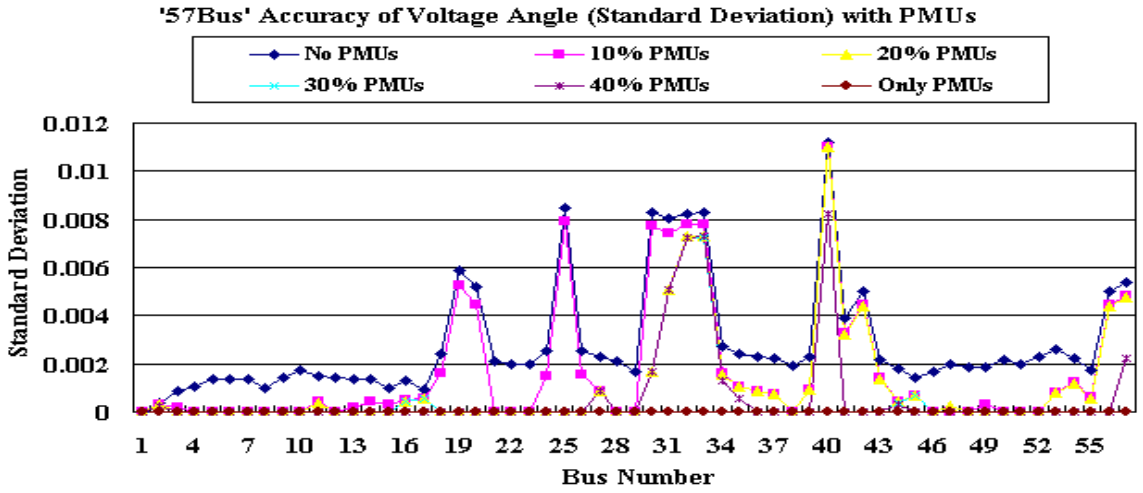

Figure 23. Voltage Angle Accuracy of IEEE57 Bus System with PMUs

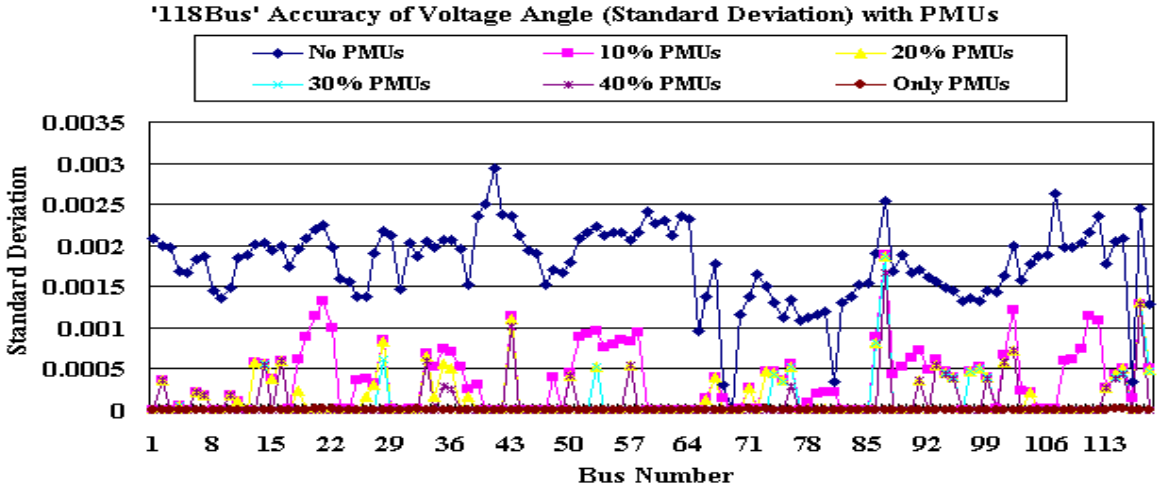

Figure 24. Voltage Angle Accuracy of IEEE118 Bus System with PMUs

Average valued S.D.(Standard Deviation) of each variables are shown in Figures 25~28 for voltage magnitudes, and in Figures 29~32 for voltage angles.

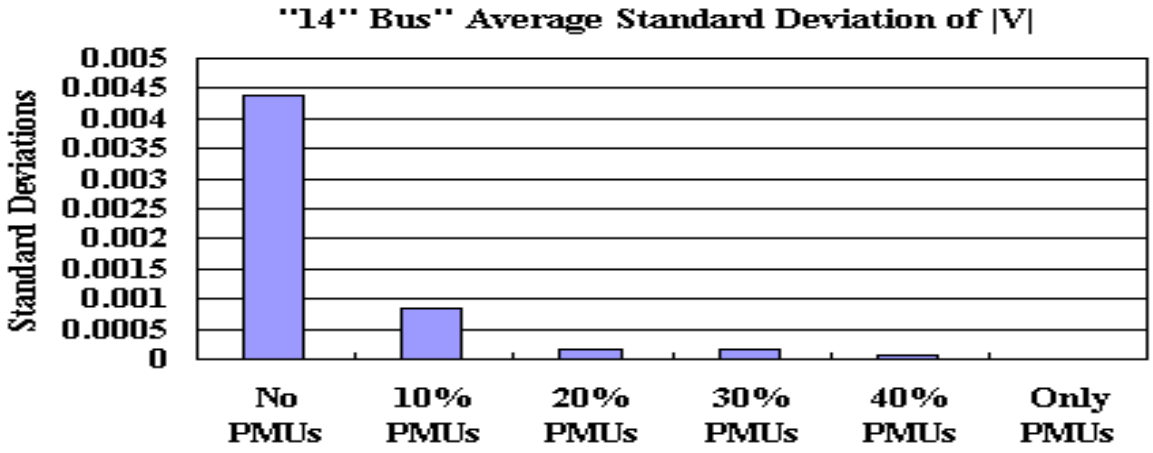

Figure 25. Average |V| Standard Deviation of IEEE14 Bus System

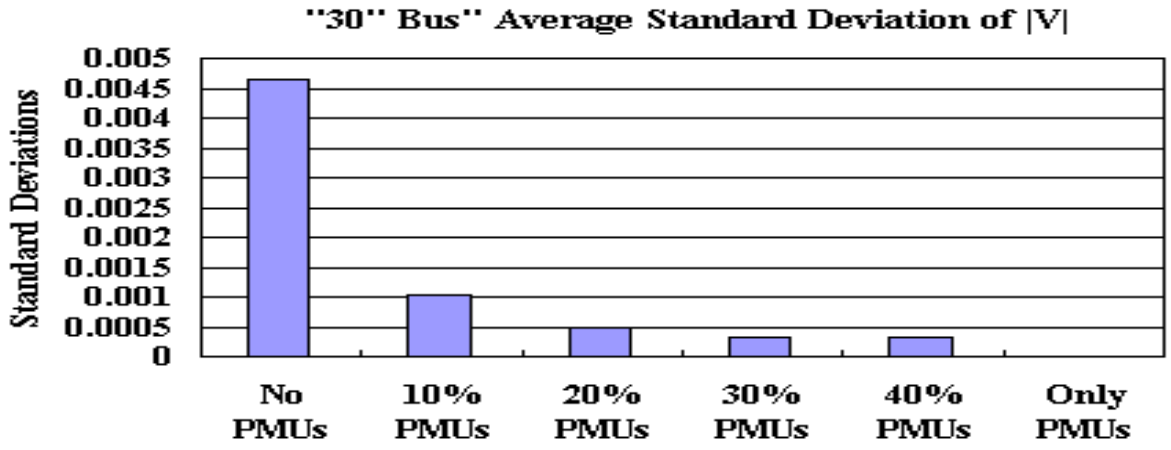

Figure 26. Average |V| Standard Deviation of IEEE30 Bus System

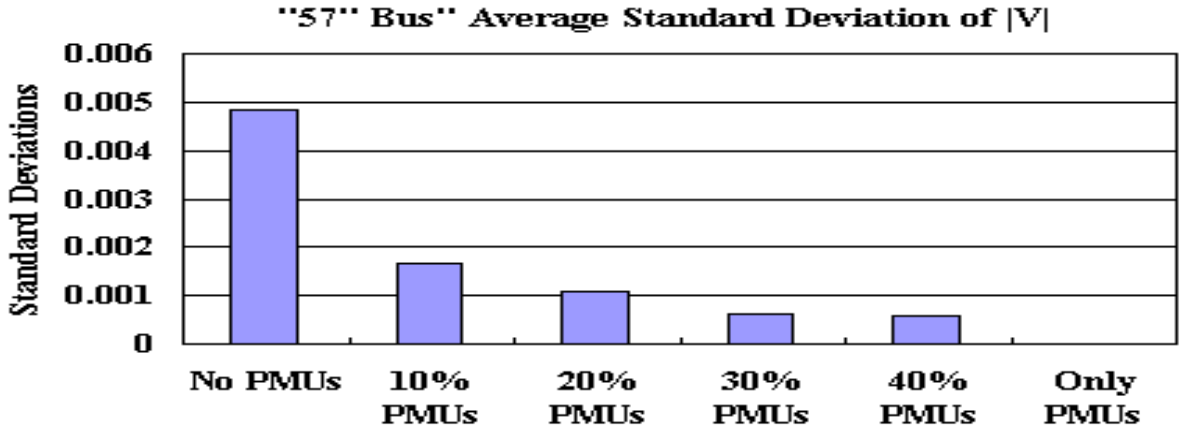

Figure 27. Average |V| Standard Deviation of IEEE57 Bus System

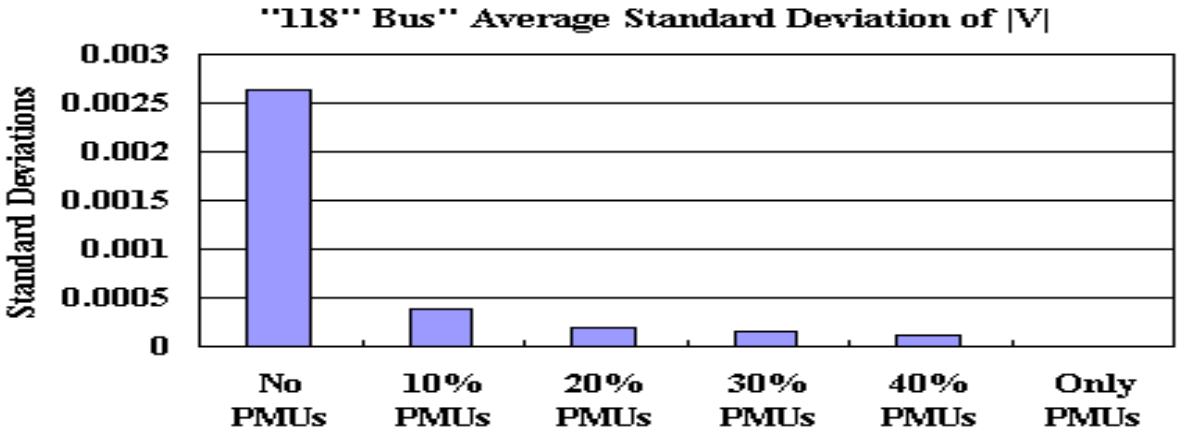

Figure 28. Average |V| Standard Deviation of IEEE118 Bus System

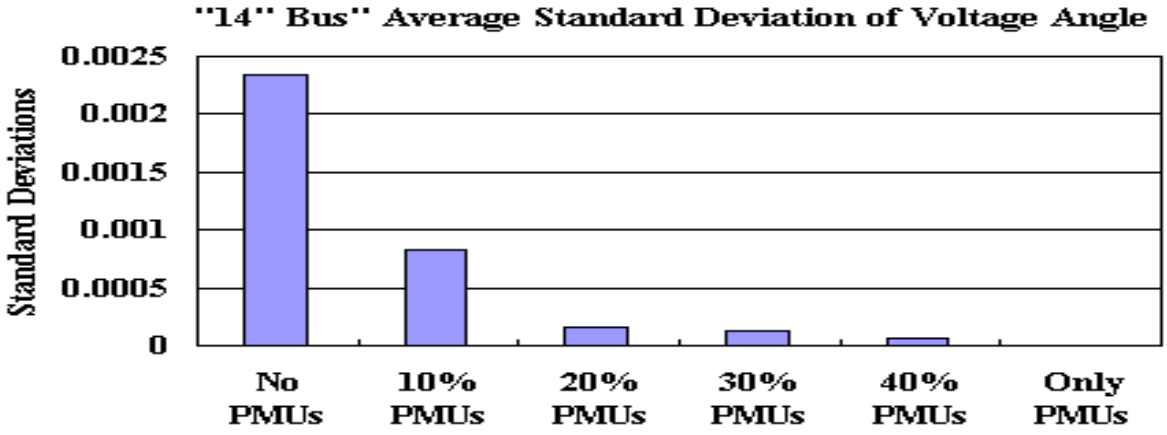

Figure 29. Average Voltage Angle Standard Deviation of IEEE14 Bus System

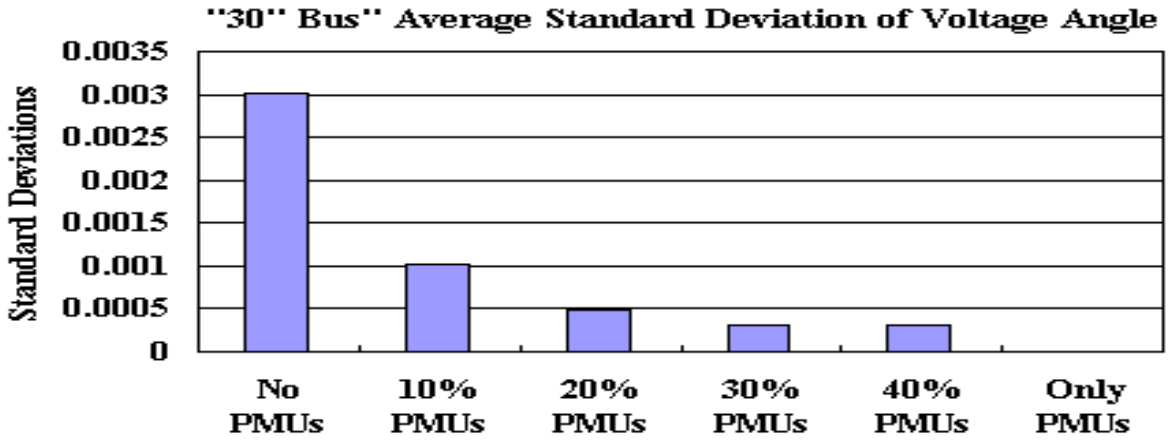

Figure 30. Average Voltage Angle Standard Deviation of IEEE30 Bus System

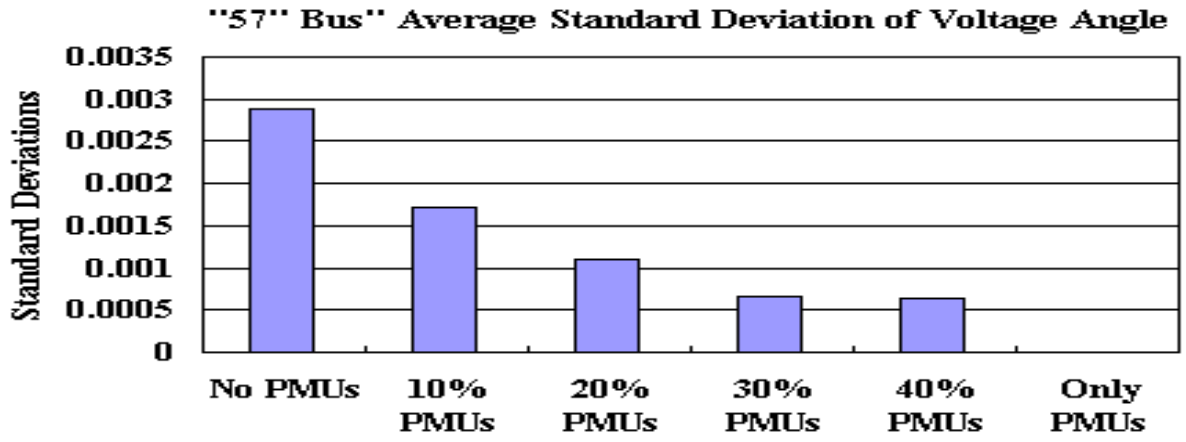

Figure 31. Average Voltage Angle Standard Deviation of IEEE57 Bus System

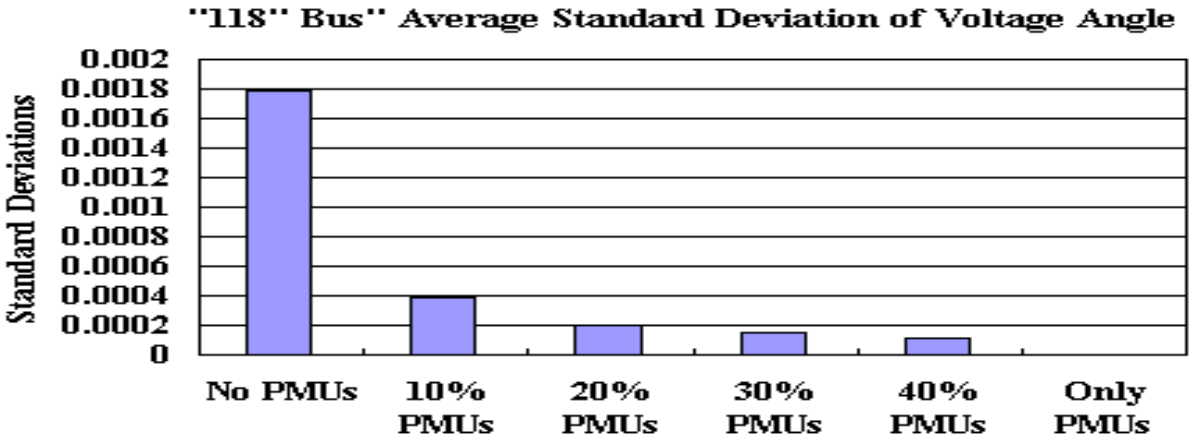

Figure 32. Average Voltage Angle Standard Deviation of IEEE118 Bus System

Table 12. Average Error Standard Deviations of the Estimated Variables

Type of Variables	Type of IEEE Bus Systems	Case 1	Case 2	Case 3	Case 4	Case 5	Case 6
		No PMUs	10% PMUs	20% PMUs	30% PMUs	40% PMUs	Only PMUs
Voltage Magnitude ($\|V\|$)	14 Bus	0.0043741 (100%)	0.0008449 (19.31%)	0.0001727 (3.95%)	0.0001497 (3.42%)	0.0000810 (1.85%)	0.0000055 (0.13%)
	30 Bus	0.0046548 (100%)	0.0010444 (22.43%)	0.0004986 (10.70%)	0.0003240 (6.96%)	0.0003229 (6.94%)	0.0000042 (0.09%)
	57 Bus	0.0048461 (100%)	0.0016503 (34.05%)	0.0010682 (22.00%)	0.0006291 (12.98%)	0.0005864 (12.12%)	0.0000063 (0.13%)
	118 Bus	0.0026439 (100%)	0.0003763 (14.23%)	0.0001916 (7.25%)	0.0001522 (5.76%)	0.0001110 (4.20%)	0.0000045 (0.17%)
Voltage Angle (δ)	14 Bus	0.0023332 (100%)	0.0008298 (35.56%)	0.0001555 (6.66%)	0.0001311 (5.62%)	0.0000618 (2.65%)	0.0000027 (0.11%)
	30 Bus	0.0030143 (100%)	0.0010244 (33.98%)	0.0004918 (16.3%)	0.0003182 (10.56%)	0.0003171 (10.52%)	0.0000032 (0.11%)
	57 Bus	0.0028824 (100%)	0.0017072 (59.23%)	0.0011105 (38.53%)	0.0006607 (22.92%)	0.0006291 (21.82%)	0.0000054 (0.19%)
	118 Bus	0.0017892 (100%)	0.0003832 (19.31%)	0.0001940 (3.95%)	0.0001542 (3.42%)	0.0001122 (1.85%)	0.0000041 (0.13%)

The percentage values in the Table 12 mean that how the S.D. values at each cases are decreased compared to the S.D. of ‘Case 1’ which are forced to be set as 100% for each systems. In the IEEE118 bus system for example, the S.D. of the estimated voltage magnitude is approximately 0.00264 (Set to be 100%) when there is no PMUs, but after adding 10% of PMUs to the system, it becomes nearly 0.000376 (14.23%). It means that ‘85.77%’ of the S.D. of ‘Case 1’ is decreased by adding only 10% of PMUs. In case of ‘Only PMUs’, it becomes nearly zero, such as 0.000006 which is far less than the ‘No PMUs’ case. The interesting thing is that the rates of percent decreasing are maximum at ‘Case 2’ which has 10% of PMUs. Therefore, this result shows that the most cost effective way of installing PMUs is to add them to the system around 10% of the total bus numbers, while decreasing the errors of the estimated variables.

CHAPTER V
MULTI-AREA STATE ESTIMATION

5.1 Current Method of Multi-Area State Estimation

After the deregulation of the power systems, state estimation solution for a large scaled interconnected system is needed. Several kinds of research for the multi-area methods of the state estimation are done earlier in [36]-[44]. Different kinds of analysis for the system network by nodes [36], tie-lines [37],[38],[39] or the structure of the gain matrix [40] are suggested. However, their ideas are mainly centered on the computing time, memory issues, and exchange of data between areas. Recently, multi-area state estimation including boundary measurements and requiring no iterations between the local and central estimators is proposed in [45]. The existing multi-area state estimation method is briefly introduced in this section mostly based on [45], and new proposed strategy is discussed next.

Consider a large power system including several local areas. In each areas, the buses are classified into three different types of buses. Supposing that the area i is taken as an example, their definitions are following:

1) Internal bus : All of whose neighbors are belong to the area i
2) Boundary bus : Whose neighbors are area i internal buses and at least one boundary bus from another area.
3) External bus : Which is a boundary bus of another area with a connection to at least one boundary bus in area i

After excluding the voltage angle at the reference bus, the state vector for the area i is given by, $x_i = \left[x_i^{b^T}, x_i^{\text{int}^T}, x_i^{ext^T} \right]^T$ .Where $x_i^{b^T}$ is the state vector for the boundary buses, $x_i^{\text{int}^T}$ is for the internal buses, and $x_i^{ext^T}$ is for the external buses. This defined state vector of the voltage magnitudes and angles is for the first level state estimation. The second level state estimation includes another variables, the synchronized phase angles of the slack buses in each areas. The second level estimator coordinates the results of the individual

local area estimation, and make sure that all bad data related to the boundary measurements are identified and removed. The state vetor to be estimated in this stage is defined as:

$$x_s = [x^{b^T}, u^T]^T \tag{5.1}$$

where,

$x^{b^T} = [x_1^{b^T}, x_2^{b^T}, \cdots, x_n^{b^T}]^T$,

$u^T = [u_2, u_3, \cdots, u_n]^T$

When the reference area is arbitrarily chosen to be area 1 with $u_1 = 0$, u_i represents a voltage angle of the slack bus of the ith area with respect to the slack bus of area 1. While processing the first and second level state estimations, a WLS state estimation method is used. The central coordinator receives GPS based phasor measurement data and raw measurement data from area boundary buses. These data are used in second level state estimation to get an unbiased solutions for the whole system state. The measurement vector z is given by:

$$z_s = [z_u{}^T, z_{ps}{}^T, \hat{x}^{b^T}, \hat{x}^{ext^T}]^T \tag{5.2}$$

where,

1) z_u : Boundary measurement vector.

2) z_{ps} : GPS synchronized phasor measurement vector.

3) $\hat{x}^b$: Boundary state variables estimated by individual area state estimation.

4) $\hat{x}^{ext}$: external state variables.

The central coordinator takes those values as pseudo-measurements. The measurement model is then be given by:

$$z_s = h_s(x_s) + e_s \tag{5.3}$$

The covariance of these measurements can be obtained from the covariance matrix of the state for individual areas. From the (4.3), this matrix is equal to the inverse of the gain matrix related to that area's WLS state estimator. For the effectiveness of the coordinator estimation, synchronized phasor measurements provide the measurement redundacy effectively, while improving the quality of the estimation. The largest normalized residual

test is carried out, in both the individual area SE and the coordinator SEto detect and identify the bad data.

The main idea of this formulation is to allow each local estimator to remain completely independent in the first level and let the first stage results be coordinated by an independent central entity in the second level.

5.2 Proposed Method for Multi-Area State Estimation

The multi-area state estimation method presented in the previous section utilizes PMU measured voltage angles while accomplishing the second level state estimation. Which means that the synchronized voltage angles at slack bus in each areas are added to the measurement vector. However, those are not the only measurement data from a PMU. Single PMU can measure a voltage and currents with magnitudes and phasors. In this section, an upgraded method for multi-area state estimation with all the measurement data from PMU is introduced.

The method of incorporating PMU measurements to the conventional state estimation is explained in detail in chapter II. Considering the the second stage SE, the measurement vector z_s can have all the measurement data from PMU. The measurement vector from PMU can be expressed as z_{pmu} :

$$z_{pmu} = [z_{|v|}{}^T, z_{angle}{}^T, z_c{}^T, z_d{}^T]^T \tag{5.4}$$

Total measurement vector z_s can be expressed as:

$$z_s = [z_u{}^T, z_{pmu}{}^T, \hat{x}^{b^T}, \hat{x}^{ext^T}]^T \tag{5.5}$$

$$= [z_u{}^T, z_{|v|}{}^T, z_{angle}{}^T, z_c{}^T, z_d{}^T, \hat{x}^{b^T}, \hat{x}^{ext^T}]^T$$

The variable vector x_s in the second stage is composed of the variables in the boundary buses, PMU located buses, and neighboring buses to the PMU located buses. Therefore, the x_s can be expresssed as:

$$x_s = [x^{b^T}, x_{pmu}{}^T]^T \tag{5.6}$$

Table 13. Various Measurement Types with PMU

Measurement Type	Measurement
Power Injection	Pinj (Real Power Injection)
	Qinj (Reactive Power Injection)
Power flow	Pflow (Real Power Flow)
	Qflow (Reactive Power Flow)
Voltage from PMU	|V| (Voltage Magnitude)
	V_{angle} (Voltage Angle)
Current from PMU	C_{ij} (Real Part of Current)
	D_{ij} (Reactive part of current)
Estimated Result $\hat{x}^b$	|V| (Result of Boundary Bus from First Level Estimation)
	V_{angle} (Result of Boundary Bus from First Level Estimation)
Estimated Result $\hat{x}^{ext}$	|V| (Result of External Bus from First Level Estimation)
	V_{angle} (Result of External Bus from First Level Estimation)

There are totally 12 measurement types in the second level state estimation as shown in Table 13. Simulation works of this method is carried out in the next section. The only difference with the existing method is that the central coordinator SE has more measurements data from PMU. As expected, the accuracy of the estimated results of this method is improved by including current measurements which has small error standard deviations.

5.3 Simulation Example of IEEE14 Bus System

This system is arbitrariliy divided by two areas. Area 1 has 5 buses (1,2,3,4,5) and area 2 has 9 buses (6,7,8,9,10,11,12,13,14). Figure 33 shows the diagram and measurement placement of the integrated system. Figures 34~35 depict the segmented area 1 and area 2. Lastly, Figure 36 illustrates the buses which has to be estimated at the second level, and measuremet placement for that.

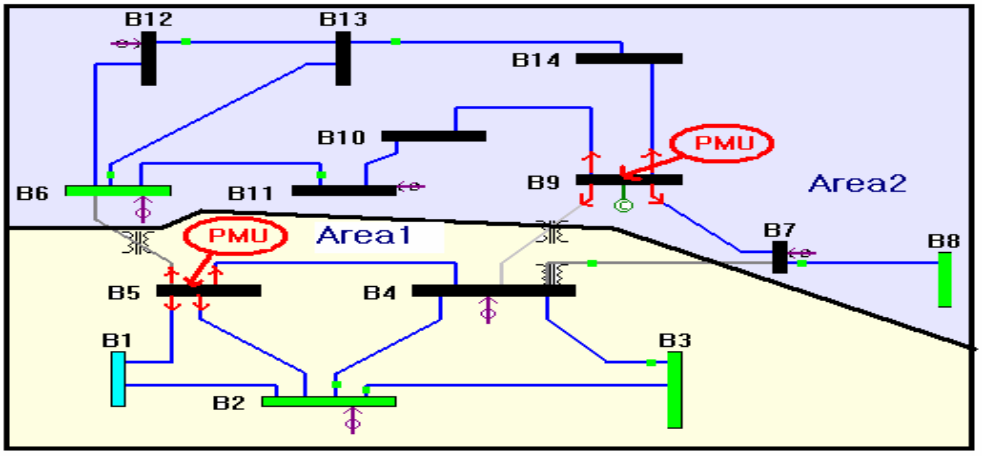

Figure 33. Diagram and Measurement Placement of Integrated System

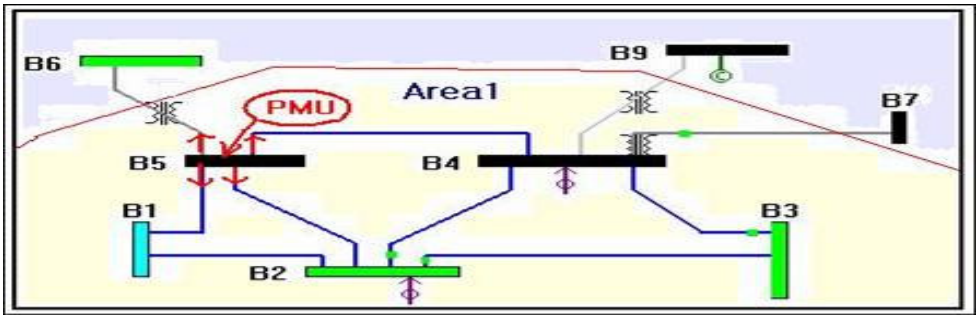

Figure 34. Diagram and Measurement Placement of Area 1

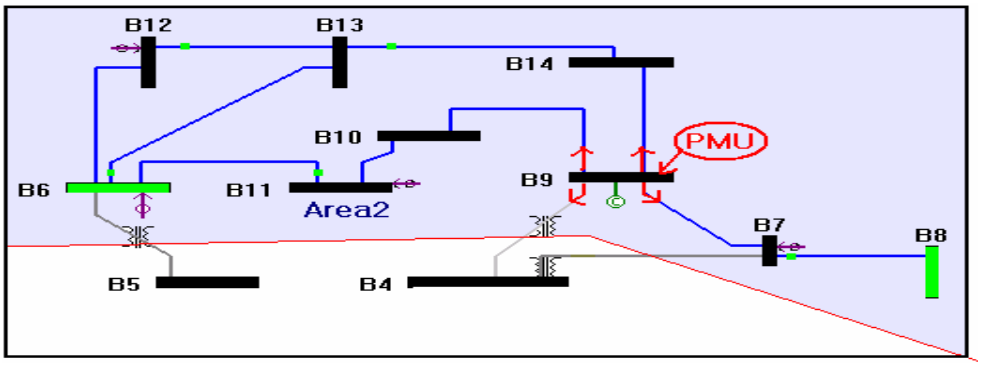

Figure 35. Diagram and Measurement Placement of Area 2

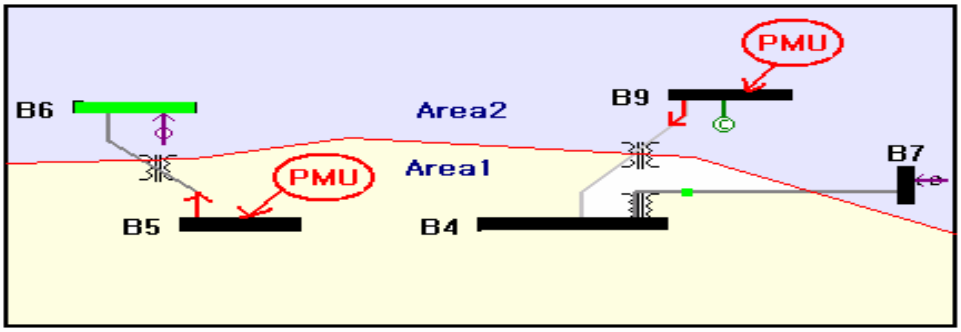

Figure 36. Second Level Estimation with Boundary Buses

Table 14 indicates the types and number of measurements and the error standard deviations for them. Gaussian errors are imposed to every measurement for the test from the exact values. Measurement data for the second level state estimation has boundary and external bus measurement variables which are estimated from the first level estimator. The gaussian standard deviations for the voltages and currents are small compared to the power injection and power flow measurement cases.

Table 14. Type, Number, and Error S.D. for Different Estimation Levels

	Power inj.	Power flow	|V|	Voltage Angle	Real Current	Reactive Current	Boundary (|V|, δ)	External (|V|, δ)
Integrated	12	18	2	2	8	8		
First level (Area1)	4	8	1	1	4	4		
First level (Area2)	8	10	1	1	4	4		
Second level	6	2	2	2	8	8	10	10
Gaussian error S.D.	0.01	0.008	0.004	0.0001	0.001	0.001	*Diag-* $(G_i^{-1}(i,i))$	*Diag-* $(G_i^{-1}(i,i))$

The results of the estimation for the different levels are summarized in Table 15. The objective functions of each cases are quite below the chi-squares limits, and the largest normalized residuals are also far below the criteria '3.0'. The result of this example indicates that the estimation is carried out successfully by two level estimation method with PMUs while including current measurements data.

Table 15. Estimation Results of IEEE14 Bus System

	Degree of Freedom	Chi-squares Limit	Objective Function J(x)	Largest r^N
Integrated	21	38.93	23.38	1.7791
Area1	6	16.81	2.52	1.3218
Area2	6	16.81	9.09	1.8095
Second-level	24	42.98	33.25	2.1457

Again, this method is tested for the bad data case, when there's a bad data in real power injection measurement at bus 6. The value of the Pinj(6), which was originally '-0.016', is replaced by '2' as a bad data. Then, the estimation with WLS method is fulfilled out by two levels. Figure 37 depicts the diagram with bad data location.

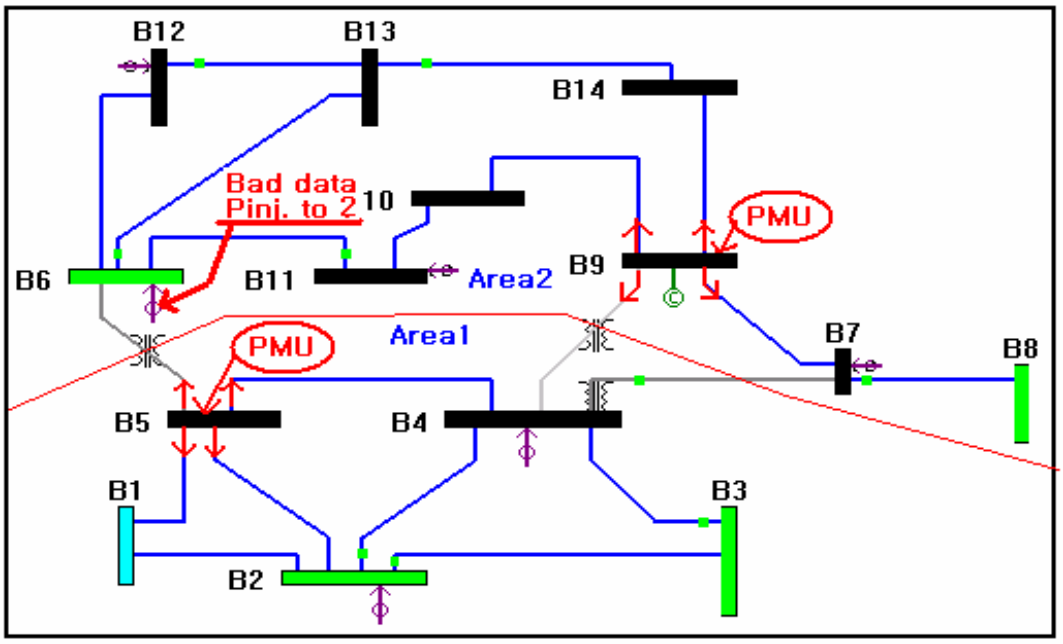

Figure 37. Diagram of IEEE14 Bus System with Bad Data

Tables 16-17 are the chi-squares and the largest normalized residual test results of state estimation in area 2 at the first level estimation.

Table 16. State Estimation Results of Area 2 with Bad Data

Degree of Freedom	Chi-squares Limit	Objective Function J(x)
6	16.81	4.03

Table 17. Sorted Normalized Residuals of Area 2 Estimation

Measurement Type	Largest Normalized Residual (r^N)
Real part of current (9,10)	1.8095
Imaginary part of current (9,7)	1.8073
Real part of current (9,14)	1.6774
:	:

Table 18. State Estimation Results of the Second Level with Bad Data

Degree of Freedom	Chi-squares Limit	Objective Function J(x)
24	42.98	27965

Table 19. Sorted Normalized Residuals of the Second Level Estimation

Measurement Type	Largest Normalized Residual (r^N)
Real power injection (6)	146.43
Real part of current (5,6)	117.54
Reactive power injection (6)	94.3880
:	:

Tho objective function value ‘4.03’ is far below the chi-squares limit ’16.81’, and the largest normalized residual is ‘1.8095’ at real current measurement (9,10). Therefore, the estimator failed to detect and identify the bad data measurement, Pinj(6) at the first level local estimation. It is because that the bad data is belong to a critical measurement at this stage. However, the coordinator SE successfully detect and identify the bad data in Tables 18-19. The objective function value ‘27965’ is over the chi-squares limit, and the largest normalized residual value is 146.43 at Pinj(6).

Example of IEEE14 bus system is tested in this section, The two-level estimation is accomplished successfully, and the benefits of the coordinator SE is investigated by adopting a bad data at Pinj(6). Only the second level estimator could detect the bad data at this time with the help of the measurement redundancy.

5.4 Simulation Example of IEEE118 Bus System

More larger power system is tested this time with same method with the IEEE14 bus case. This system is arbitrariliy divided by nine areas with 9 PMUs at each areas. Figure 38 shows the area segments and the PMU placements.

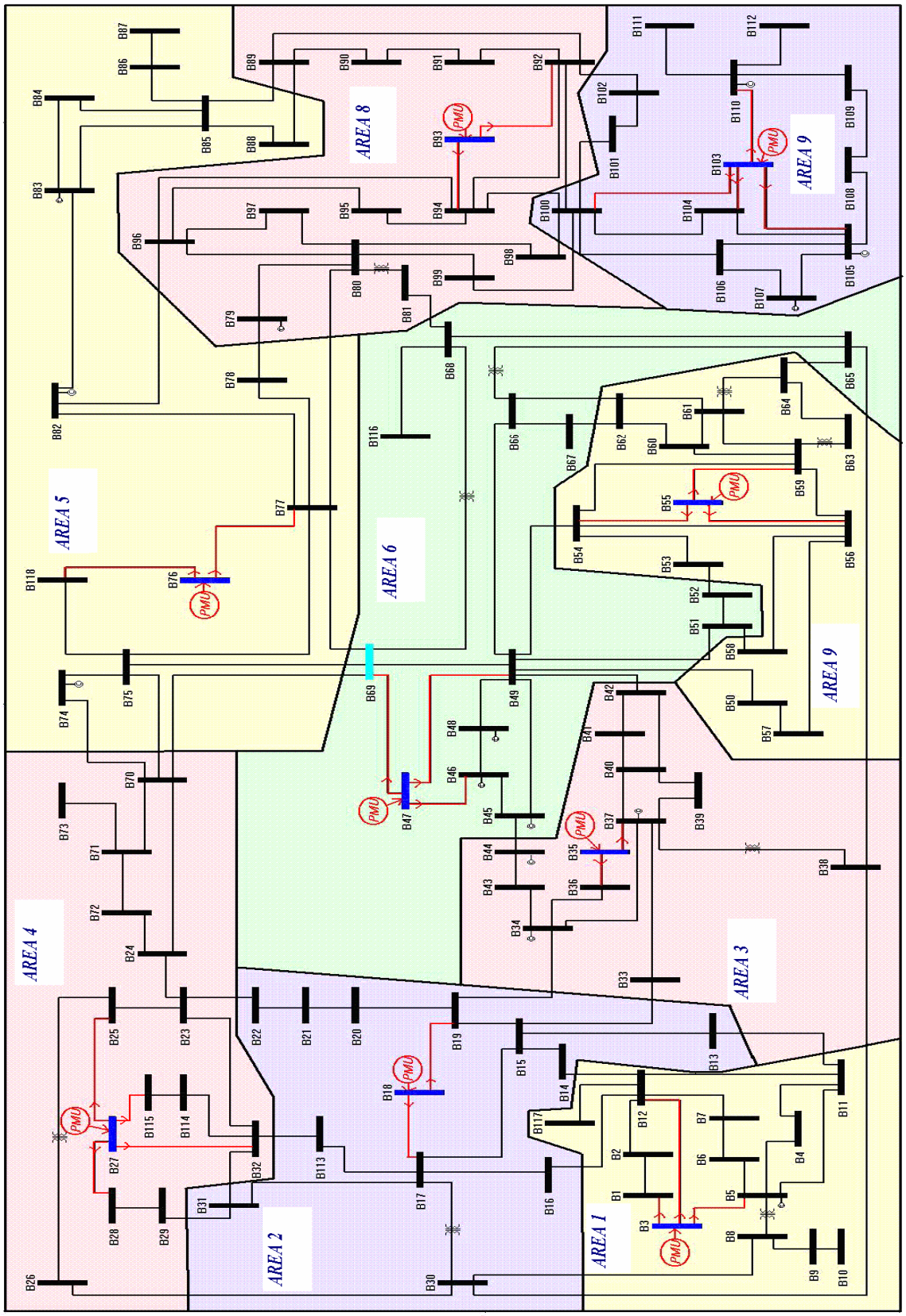

Figure 38. Diagram and PMU Placement of IEEE118 Bus System

Tables 20-21 illustrate the number of different bus types, number of measurements, and error standard deviations for the IEEE118 bus system.

Table 20. Number of Bus Types and PMUs for Different Estimation Levels

	Area1	Area2	Area3	Area4	Area5	Area6	Area7	Area8	Area9
Total Buses	13	13	12	14	13	13	13	14	13
Internal Buses	10	4	7	9	6	4	11	5	7
Boundary Buses	3	9	5	5	7	9	2	9	6
External Buses	4	10	6	7	6	13	4	8	6
Slack Bus Number	3	18	35	27	76	47	103	93	55
Voltage Meas. (PMU)	1	1	1	1	1	1	1	1	1
Current Meas. (PMU)	3	2	2	4	2	3	4	2	3

Table 21. Type, Number, and Error Standard Deviation for Different Levels

	Power Inj.	Power Flow	|V|	Voltage Angle	Real Current	Reactive Current	Boundary (|V|,Angle)	External (|V|,Angle)
Integ-rated	110	274	9	.	.	.	.	.
Area1	6	8	1	.	.	.	.	.
Area2	18	30	1	.	.	.	.	.
Area3	10	26	1	.	.	.	.	.
Area4	10	32	1	.	.	.	.	.
Area5	14	28	1	.	.	.	.	.
Area6	18	42	1	.	.	.	.	.
Area7	4	30	1	.	.	.	.	.
Area8	18	30	1	.	.	.	.	.
Area9	12	28	1	.	.	.	.	.
Second-level	110	48	9	9	25	25	110	128
Gaussian (S.D)	0.01	0.008	0.004	0.00001	0.001	0.001	*Diag-* $(G_i^{-1}(m,m))$	*Diag-* $(G_i^{-1}(m,m))$

The results of the WLS of the integrated and two level state estimation is summarized in Table 22. It has chi-squares test result and largest normalized residual test results. All the values of the objective function are below the chi-squares limit and the largest normalized residual values are also below the criteria '3.0'.

Table 22. State Estimation Results of IEEE118 Bus System

	Integ-rated	Area1	Area2	Area3	Area4	Area5	Area6	Area7	Area8	Area9	Second-level
Degree of Freedom	368	14	24	16	18	24	8	16	32	26	348
Chi-Squares Limit	404.04	29.14	42.98	32.00	34.81	42.98	20.09	32.00	53.49	45.64	412.30
Objective Function J(x)	113.69	6.62	6.66	4.94	9.77	6.18	12.59	3.73	11.09	10.98	324.68
Largest r^N	2.64	2.10	2.13	1.79	1.97	1.72	2.34	1.57	2.09	2.18	2.87

Then, a test is conducted for the bad data case. Pinj(44) is changed from '-0.154' to '1' as a bad data in Figure 39.

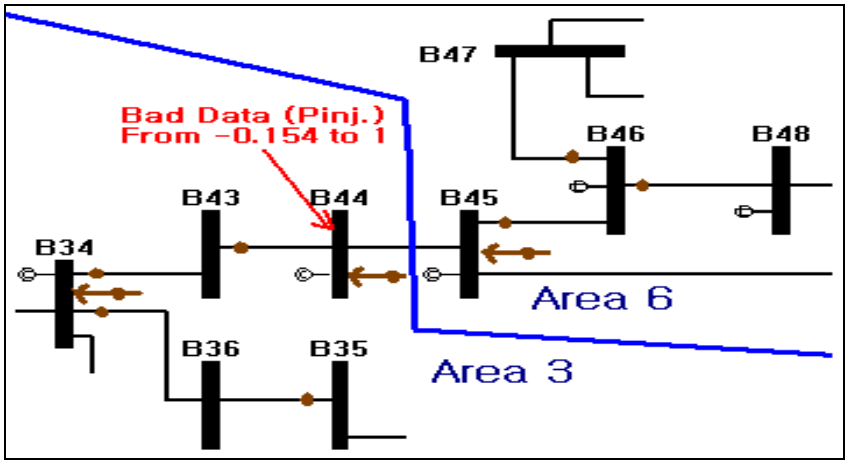

Figure 39. Diagram of Area 3 and Area 6 with Bad Data

Pinj(44) is a critical measurement for the area 3 local estimator. Therefore, the first level estimation can't detect the bad data. Tables 23-24 have the results of the area 3 estimation. Two tests indicates that there is no bad data at this level of estimation.

Table 23. State Estimation Results of Area 3 with Bad Data

Degree of Freedom	Chi-square limit	Objective function J(x)
16	32.00	4.94

Table 24. Sorted Normalized Residuals of Area 3 Estimation

Measurement Type	Largest normalized residual (r^N)
Reactive Power Flow (39,40)	1.79
Reactive Power Flow (37,40)	1.73
Reactive Power Flow (37,49)	1.67
:	:

However, the second level estimator detects and identifies the bad data exactly. Table 25 tells the objective function values is quite over the chi-squares limit, and Table 26 shows that the exact bad data is the Pinj(44) which has the largest normalized residual value.

Table 25. State Estimation Results of the Second Level with Bad Data

Degree of Freedom	Chi-squares Limit	Objective Function J(x)
348	412.30	10586

Table 26. Sorted Normalized Residuals of the Second Level Estimation

Measurement Type	Largest normalized residual (r^N)
P_{inj} (44)	77.9204
External angle (45)	69.364
Boundary angle (45)	47.978
:	:

By two simulation examples, the proposed multi-area state estimation method is tested and analyzed. In case of that the mesurement on the boundary bus is bad and is critical, the second level estimator could detect it with the PMUs while the first level state estimator failed to detect it.

CHAPTER VI
CONCLUSIONS AND FUTURE WORK

6.1 Conclusions

In chapter II the way of incorporating the PMU data to the conventional measurement set is discussed. A PMU can measure voltage and current with magnitude and phasors. The current measurement is implemented to the measurement set as a rectangular form. Equations for the added measurements are illustrated in detail including the elements of the Jacobian matrix. It is expected that those PMU measured data improve the measurement redundancy and accuracy, due to the small error standard deviations of PMU.

A linear formulation of the state estimation is investigated in chapter III, using only PMU measured data. All the variables and measurements are reformed as a rectangular form, and they are treated separately during the estimation process. This linear formulation of the PMU data can produce the estimation result by a single calculation not requiring any iterations. Several examples are tested including bad data detection case. If a mesaurement set having only PMU data is exist in the real world, the improvement of the computation time and accuracy is expected, with the linear formulation of the state estimation.

Chaper IV examines the benefits of using PMU, which improves the accuracy of the estimated variables. Six cases are tested while gradually increasing the number of PMUs which are added to the measurement set. With the help of advanced accuracy of PMU, it was seen that the estimated accuracy is also gradually increase. One of the interesting thing is that the accuracy improves most effectively when the number of implemented PMUs are around ‘10%’ of the system buses. It is proved that the quality of the estimation is bettered by adopting PMU data to the measurement set.

Lastly, chapter V surveys a multi-area state estimation process and proposes advanced method applying all the measurements of PMU to the two level estimator. This method is tested by two examples. The test results show that the first level state estimation at each area is completely independent as a local estimator. This estimated results of all the boundary and external buses are sent to the central coordinator for the second level

estimation, and there's no iterations between the local estimator and the central entity. In case of imposed bad data to a boundary bus, the local estimator fails to detect it while the second level estimator exactly detects and identifies it. As a conclusion, the synchronized measurements from PMU, makes possible the multi-area state estimation for a large power system, and improves the accuracy and quality of the estimation results.

6.2 Future Work

The work done in this report indicates that PMU has many benefits in the state estimation process. If the PMU is installed through the entire system, the linear formulation of the state estimation can be used which has fast execution time and improved accuracy. While the information about the interconnected different areas is becoming more important, a multi-area state stimation for a huge size of system is needed nowadays. Furthermore, each area should install PMU for the synchronization, and communicate between the different areas and central coordinator, while the concerned network areas are becoming more larger. By doing so, the multi-area state estimation for a large network system can be done.

In order to efficiently install PMUs to the existing system, a research for the optimal PMU placement is needed. The way of deploying the PMUs would determine improvement level of the accurcy and the cost. Also, an analysis for the cost effects of adding more PMU is required.

REFERENCES

[1] N. I. Voropai, "Investments and development of electric power industry in market environment", in *Proc. Int. Power System Technology Conf.*, Kumning, China, October 2002.

[2] W. J. Lee, and C. H. Lin, "Utility deregulation and its impact on the industrial power systems", in *IEEE Industrial and Commercial Power Systems Technical Conf. Record*, Philadelphia, PA, May 1997.

[3] G. J. Miranda, "Be Prepared! [power industry deregulation]", *IEEE Industry Applications Magazine*, vol. 9, no. 2, March/April 2003.

[4] G. M. Huang, and J. Lei, "Measurement design of data exchange for distributed multi-utility operation", in *IEEE Power Engineering Society Winter Meeting*, New York, NY, January 2002.

[5] E. Iwata, "Report faults Ohio utility", *USA Today*, pp. 1A , November 20, 2003.

[6] M. Rice, and G. T. Heydt, "Phasor measurement unit data in power system state estimation", *PSERC Intermediate Project Report Enhanced State Estimator Project S-22*, April 2005.

[7] J. S. Thorp, A. G. Phadke, and K. J. Karimi, "Real time voltage-phasor measurements for static state estimation", *IEEE Transactions on Power Apparatus and Systems*, vol. 104, pp. 3098-3104, November 1985.

[8] R. Zivanovic, and C. Cairns, "Implementation of PMU technology in state estimation: An overview", *IEEE AFRICON 4th*, University of Stellenbosch, South Africa, September 1996.

[9] A. G. Phadke, "Synchronized phasor measurements ~ a historical overview", in *Proc. of the Transmission and Distribution Conference and Exhibition in Asia/Pacific*, Yokohama, Japan, October 2002.

[10] I. Kamwa, and R. Grondin, "PMU configuration for system dynamic performance measurement in large multiarea power systems", *IEEE Transactions on Power Systems*, vol. 17, pp. 385-394, May 2002.

[11] W. Lewandowski, J. Asoubib, and W. J. Klepczynski, "GPS: primary tool for time transfer", *Proc. of the IEEE*, vol. 87, pp. 163-172, January 1999.

[12] Y. Ota, and H. Ukai, "PMU based midterm stability evaluation of wide-area power system", in *Proc. of the Transmission and Distribution Conference and Exhibition in Asia/Pacific*, Yokohama, Japan, October 2002.

[13] K. S. Cho, J. R. Shin, and S. H. Hyun," Optimal placement of phasor measurement units with GPS Receiver", in *IEEE Power Engineering Society Winter Meeting*, Columbus, Ohio, January 2001.

[14] X. Bei, Y. Yoon, and A. Abur, "Optimal placement and utilization of phasor measurements for state estimation", in *Proc. of the 15th Power Systems Computation Conf.*, Liege, Belgium, August 2005.

[15] G. B. Denegri, M. Invernizzi, F. Milano, M. Fiorina, and P. Scarpellini, "A security oriented approach to PMU positioning for advanced monitoring of a transmission grid", in *Proc. of the Int. Conference on Power System Technology*, Kuming, China, October 2002.

[16] B. Milosevic, and M. Begovic, "Nondominated sorting genetic algorithm for optimal phasor measurement placement", *IEEE Transactions on Power Systems*, vol. 18, pp. 69-75, February 2003.

[17] E. Handschin, F. C. Schweppe, J. Kohlas, and A. Fiecher, "Bad data analysis for power system state estimation", *IEEE Transactions on Power Apparatus and Systems*, vol. 94, pp. 329-337, March/April 1975.

[18] P. Zarco, and A. Exposito, "Power system parameter estimation:a survey", *IEEE Tranactions on Power Systems*, vol. 15, pp. 216-222, February 2000.

[19] G. N. Korres, and G. C. Contaxis, "A heuristic approach for the selection of state estimator measurement schemes", in *6th Mediterranean Electrotechnical Conf. Proc.*, Ljubljana, Yugoslavia, May 1991.

[20] F. Schweppe, J. Wildes, and D. Rom, "Power system static state estimation: Parts I,II, and III", *IEEE Transactions on Power Apparatus and Systems*, vol. 89, pp. 120-135, January 1970.

[21] A. Abur, and A. G. Exposito, *Power System State Estimation: Theory and Implementation*, New York: Marcel Dekker, 2004.

[22] J. Grainger, and W. Stevenson, *Power System Analysis*, New York: McGraw-Hill Inc., 1994.

[23] O. Alsac, N. Vempati, B. Stott, and A. Monticelli, "Generalized state estimation", *IEEE Transactions on Power Systems*, vol. 13, pp. 1069-1075, August 1998.

[24] K. A. Clements, G. R. Krumpholz, and P.W. Davis, "Power system state estimation with measurement deficiency: An algorithm that determines the maximal observable subnetwork", *IEEE Transactions on Power Apparatus and Systems*, vol. 101, pp. 3044-3052, September 1982.

[25] G. R. Krumpholz, K.A. Clements, and P. W. Davis, "Power system observability: A practical algorithm using network topology", *IEEE Transactions on Power Apparatus and Systems*, vol. 99, pp. 1534-1542, July/August 1980.

[26] A. Monticelli, and Felix F. Wu, "Network observability: Identification of observable islands and measurement placement", *IEEE Transactions on Power Apparatus and Systems*, vol. 104, pp. 1035-1041, May 1985.

[27] A. Monticelli, and Felix F. Wu, "Network observability: Theory", *IEEE Transactions on Power Apparatus and Systems*, vol. 104, pp. 1042-1048, May 1985.

[28] E. Handschin, F. C. Schweppe, J. Kohlas, and A. Fiecher, "Bad data analysis for power system state estimation", *IEEE Transactions on Power Apparatus and Systems*, vol. 94, pp. 329-337, March/April 1975.

[29] K. A. Clements, G. R. Krumpholz, and P. W. Davis, "Power system state estimation residual analysis: An algorithm using network topology", *IEEE Transactions on Power Apparatus and Systems*, vol. 100, pp. 1779-1787, April 1981.

[30] A. Monticelli, and A. Garcia, "Reliable bad data processing for real-time state estimation", *IEEE Transactions on Power Apparatus and Systems*, vol. 102, pp. 1126-1139, May 1983.

[31] H. M. Merrill, and F. C. Schweppe, "Bad data suppression in power system static-state estimation", *IEEE Transactions on Power Apparatus and Systems*, vol. 90, pp. 2718-2725, May 1971.

[32] A. Garcia, A. Monticelli, and P. Abreu, "Fast decoupled state estimation and bad data processing", *IEEE Transactions on Power Apparatus and Systems*, vol. 98, pp. 1645-1651, September/Octocber 1979.

[33] M. Kezunovic, A. Abur, G. Huang, A. Bose, and K. Tomosovic, "The role of digital modeling and simulation in power engineering education", *IEEE Transactions on Power Systems*, vol. 19, pp. 64-72, February 2004.

[34] A. Abur, F. Magnago, and Y. Lu, "Educational toolbox for power system analysis", *IEEE Computer Applications in Power*, vol. 13, pp. 31-35, October 2000.

[35] R. Christie, "Power System Test Archive", http://www.ee.washington.edu/research, March 3, 2005.

[36] K. A. Clements, O. J. Denison, and R. J. Ringlee, "A multi-area approach to state estimation in power system networks", in *IEEE PES Summer Meeting*, Paper C72 465-3, San Fransisco, CA, 1973.

[37] H. Kobayashi, S. Narita, and M. S. A. A. Hamman, "Model coordination method applied to power system control and estimation problems", in *Proc. of the IFAC/IFIP 4th Int. Conf. on Digital Computer Applications to Process Control*, Tokyo, Japan, August 1974.

[38] Th. Van Cutsem, J. L. Horward, and M. Ribbens-Pavella, "A two-level static state estimator for electric power systems", *IEEE Transactions on Power Apparatus and Systems*, vol. 100, pp. 3722-3732, August 1981.

[39] K. Abdel-Rahman, L. Mili, A. Phadke, J. De La Ree, and Y. Liu, "Internet based wide area information sharing and its roles in power system state estimation", in *IEEE Power Engineering Society Winter Meeting*, Columbus, Ohio, January 2001.

[40] Th. Van Cutsem, and M. Ribbens-Pavella, " Critical survey of hierarchical methods for state estimation of electric power systems", *IEEE Transactions on Power Apparatus and Systems*, vol. 102, pp. 3415-3424, October 1983.

[41] Y. Wallach, and E. Handschin, "An efficient parallel proceeding method for power system state estimation", *IEEE Transactions on Power Apparatus and Systems*, vol. 100, pp. 4402-4406, November 1981.

[42] I. O. Habiballah, "Modified two-level state estimation approach", in *IEE Proc. of Generation, Transmission and Distribution*, Atlanta, Georgia, March 1996.

[43] S. A. Arafeh, and R. Schinzinger, "Estimation algorithms for large-scale power systems", *IEEE Transactions on Power Apparatus and Systems*, vol. 98, pp. 1968-1977, November/December 1979.

[44] A. Abur, and M. K. Celik, "Multi-area linear programming state estimator using Dantzig-Wolfe decomposition", in *Proc. of the 10th Power Systems Computations Conf.*, Graz, Austria, August 1990.

[45] Liang Zhao, and Ali Abur, "A two-level state estimator for multi-ISO operation", in *Proc. of the Thirty-fifth Annual North American Power Symposium*, Rolla, Missouri, August 2003.

VITA

Name: Yeo Jun Yoon

Address: Hyundai 2Cha Apt. 101-607, Munjung-Dong 58, Songpa-Gu, Seoul, Korea, 138-200

Email Address: juni3377@naver.com

Education: B.S., Electrical Engineering, Korea University, 2002

M.S., Electrical Engineering, Texas A&M University, 2005